Spring 2007

Operation of a brushless DC drive for application in hybrid electric vehicles

James Scott Jenkins

Department:

OPERATION OF A BRUSHLESS DC DRIVE FOR APPLICATION IN HYBRID ELECTRIC VEHICLES

By

JAMES SCOTT JENKINS

A THESIS

Presented to the Faculty of the Graduate School of the

UNIVERSITY OF MISSOURI-ROLLA

In Partial Fulfillment of the Requirements for the Degree

MASTER OF SCIENCE IN ELECTRICAL ENGINEERING

2007

Approved by

Dr. Badrul H. Chowdhury, Advisor	Dr. Kelvin Todd Erickson
Dr. Keith Corzine	

ABSTRACT

One of the goals of a hybrid electric vehicle design is to improve the overall performance of the vehicle by incorporating several different power sources in such a way as to maximize the energy usage. By combining the desirable characteristics of each of the components in the system, the vehicle becomes more efficient to operate. Energy storage systems such as batteries and ultra-capacitors can be used to supply or store energy from the system when needed. The primary power source in this model will be an internal combustion engine coupled with a permanent magnet synchronous generator. The purpose of this thesis is to analyze simulation models of the power management system and coordinate these power sources to supply the needed power to a brushless DC motor which acts as part of the propulsion system of a vehicle.

The proposed hybrid consists of a generator, an ultra-capacitor and a system of buck/boost converters to boost power to the necessary voltage level to be used by the Brushless DC motor. The generator can supply large amounts of power to the system, but most generators take time to ramp up to the rated speed of the generator. The power reclaimed during regenerative breaking, cannot be reclaimed by the generator, this is done by a storage device. Ultra-capacitors are highly efficient and have a high power density, but also typically have a low energy density when compared to batteries. Combining the long duration power supply of the generator and the short duration high power supply of an ultra-capacitor allows an effective hybrid system to be built. Setting up models of each of these components and coordinating their use is the main purpose of this thesis.

ACKNOWLEGEMENTS

I would first like to thank all of my committee members for agreeing to serve on my committee. I would like to thank Dr. Chowdhury for his help during graduate school both for his guidance as my advisor and for his help in finding employment to make graduate school more affordable and diverse. I would also like to thank anyone who has been involved in any aspect of my research as I worked toward my degree.

My parents and loved ones have also been a great help to me both financially and in supporting my decision to attend graduate school. I thank them for their assistance.

TABLE OF CONTENTS

LIST OF ILLUSTRATIONS

LIST OF TABLES

1. INTRODUCTION

1.1 IMPORTANCE OF HYBRIDS/HYBRID TECHNOLOGY

Hybrid electric vehicles have been an area of interest for consumers and scientists in recent years due to the potential for high fuel efficiency and the desire to reduce pollution. There is typically some variation among the different hybrids that make them unique such as how the energy is transferred either electrically or mechanically or what type of fuel/energy sources could be used to power the hybrid. The novel aspects of the proposed hybrid described in this thesis are its use of high efficiency Brushless DC (BDC) drives used in a mostly electrical system to propel a vehicle while coordinating energy usage to get the most out of the available power sources in terms of performance. The only fossil fuel component is the assumed internal combustion engine that is mechanically coupled to a permanent magnet generator. Regeneration allows some of the vehicle's mechanical energy to be recaptured by the electrical system. Several advances in technology have allowed for better power usage in an electrical system. Ultra-capacitors are constantly being improved and can be sized appropriately for many power applications with ultra-capacitor modules including capacitor balancing [1]. Newer, more efficient batteries are being developed for shorter charging times, lighter physical weights, and higher energy densities. Different battery types have different characteristics that may be appealing for a specific application. For example, a Ni-MH would be one of the best choices for a hybrid application due to its high efficiency in charging and discharging and its high overall efficiency [2]. High efficiency BDC motors are being improved to get the most torque per amp out of any drive system.

1.2 HYBRID SYSTEM COMPONTENTS

1.2.1 Brushless DC Motor. Brushless DC motors/generators were chosen due to their high efficiency, high torque per amp capabilities, and relatively low maintenance requirements [3]. Because of their control complexity, BDC drives are greatly simplified by using *qdo* reference frame variables for their control. Using feedback on rotor position and speed, it is then possible to control the performance of the BDC drive by controlling torque or speed, depending on the desired application, in the *qdo* reference frame and then converting back to the *abc* reference frame. Power electronic switches can be used with many different control schemes to manipulate the input voltage and convert the applied dc voltage to whatever currents or voltages are needed by the BDC motor. The BDC can be operated in motor mode when needed or can be operated as a generator during braking depending on the control of the power electronics.

The physical performance of the BDC motor is dependent on physical characteristics of the motor such as stator resistances, stator inductances, number of poles, the type of motor control, and the applied dc voltage to the BDC drive. These variables are typically determined by manufacturer's specifications or lab tests.

1.2.2 Ultra-Capacitors. The ultra-capacitor uses the properties of a normal capacitor to give much larger capacitance than was previously available. The porous surface of the capacitor electrodes, coupled with the electrolytic solution between electrodes, help give the ultra-capacitor high values of capacitance. The large capacitances of ultra-capacitors are useful in the system for two main reasons: high power density when used as a power source and high capacitance to smooth out voltage ripples on the dc bus. Ultra-capacitors can be purchased with capacitance values in the

hundreds of Farads and can handle charge/discharge currents of hundreds of amps [4]. Ultra-capacitors can also have as many as a million duty cycles before breaking down [4]. Its large capacitance value and superior charging and discharging aspects make the ultra-capacitor an essential part when a quick supply of power is needed.

1.2.3 Batteries. As a primary or secondary power source, a battery can be very useful in the design of a hybrid. Batteries can be classified based on their energy density, power density, life cycle, cost, environmental cost, and type of electrochemical reaction [2]. There are many other considerations, but for determining what to use in a hybrid, the main considerations have been listed. Typically the best performing battery is also the most expensive. A lightweight, high energy battery could cost in the tens of thousands of dollars [2].

Batteries can supply large amounts of energy over an extended period of time (hours) but one of the principal drawbacks is its slow rate of charging. Batteries have an ampere-hour rating that gives an idea of how fast the battery can be safely charged and discharged. Typically the rule is to take the ampere-hour rating and divide by 10 to determine the safe charging current magnitude. Of course, all batteries are different; some have faster charging times, but those are usually a very expensive alternative especially for larger batteries.

The battery considered in this paper is the lead-acid type due to their low cost and availability. The lead-acid battery has charging times sometimes in the tens of hours and typically cannot be discharged less than approximately 80% of their rated voltage value [2]. Many lead acid battery models have been tested and models have been developed which is another significant reason for choosing lead-acid batteries over the more

expensive alternatives. Unfortunately, it was not possible to incorporate the battery model into the final hybrid design.

1.2.4 Buck/Boost Converters. Several different types of converters have been considered for implementation. The most effective design from the perspective of ease of control and coordination was found in Reference [5]. This multiple input DC-DC converter is located between the power source and the dc bus to the inverter. The purpose of the converter is to supply power from the power sources when the BDC is in motoring mode and recharge the power sources when the BDC is in generator mode (when the vehicle is braking). The converter is bi-directional; it can operate in boost mode to supply power to the dc bus or it can operate in buck mode to supply power to the power sources during breaking mode. The primary losses that occur are due to switching and conduction. Power MOSFETs have been chosen as the power electronic switch of the converters due to their low losses and high switching frequencies.

1.3 SYSTEM MODEL LAYOUT

The layout of the proposed system is shown in Figure 1.1. Each block represents a different system component. The direction of the arrows represents the direction of power flow. There are several different sub-systems of the overall system. An internal combustion engine (ICE) is connected mechanically to the permanent-magnet synchronous machine (PMSM). It is assumed that the mechanically coupled rotor speed is the only input to the PMSM generator. The output of the generator is rectified through a 3-phase rectifier to produce a dc voltage. The dc voltage output is then sent to a boost converter to supply a voltage to the dc bus when needed. The ultra-capacitor is also

interfaced through a converter that operates in boost mode to supply power to the dc bus or in buck mode to supply power back to the ultra-capacitor.

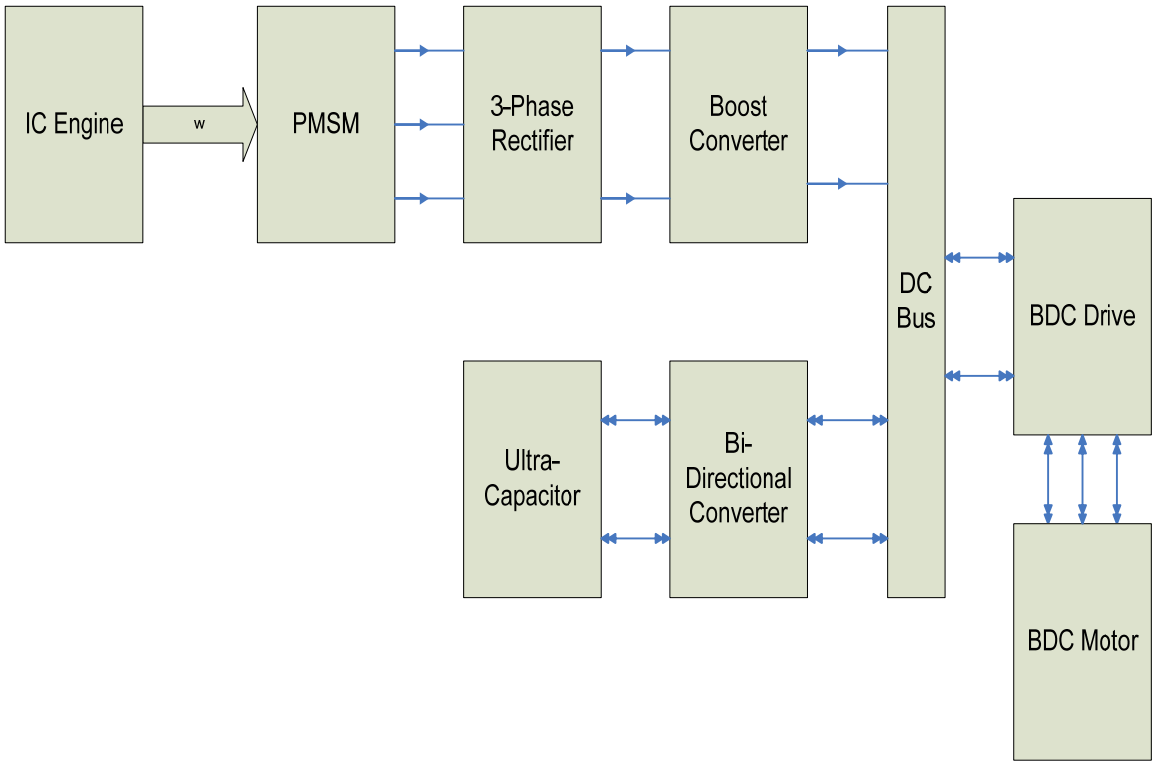

Figure 1.1. System layout

The dc bus supplies all the power to the BDC motor. By noting the direction of the arrows in the system, it can be seen that the BDC motor operates as a motor, during vehicle propulsion, and a generator, during regenerative braking. The flow of power from the ICE to the dc bus is only in one direction as the ICE cannot reclaim any power that might be created during regenerative braking. The only path for capturing any energy during braking is by use of the ultra-capacitor.

1.4 MOTIVATION

There has been a demand for more efficient hybrid vehicle drive systems for quite some time. In the U.S. where gasoline prices will fluctuate sometimes exceeding $3/gallon of gasoline, any attempt to design a more efficient, high performance vehicle should be considered to be a worthwhile pursuit. By having an electrical power system, some of the power involved in braking can be reclaimed and reused. A combination of an internal combustion engine and ultra-capacitors may be presented to show better system performance and how much more efficient a hybrid drive system can be.

In terms of performance, electric motors can provide much more transient torque and hence more acceleration than their internal combustion engine counterparts. Due to long charging times for batteries and the low energy densities of ultra-capacitors, an internal combustion engine can be used to compliment the desirable characteristics of all three of these power supplies. This is simply one version of many that can be considered for use as a hybrid while considering performance. Many people, including the automotive industry leaders, researchers, and consumers, have considered many different types of hybrids. This thesis attempts to provide performance information concerning speed control and mechanical torque loads with a BDC motor hybrid.

1.5 THESIS OUTLINE

A two power source system - a PMSM generator and an ultra-capacitor - supply power to a dc bus via a system of buck/boost converters to manage power coordination for the operation of a BDC motor tied to a dc bus. The system load is a BDC motor with a hysteresis current controlled system.

A literature review is done in Section 2 to discuss all sources used for topics concerning the power supply devices and the BDC motor. Section 3 discusses the models of individual system components and their control and operation in the system. Also discussed in section three is the operation of the buck/boost interface to the dc supply and control of the BDC machine. Section 4 consists of simulation set-up and results of different simulation scenarios. Section 5 deals with the conclusion of the completed system during various BDC motor load and commanded speeds. Also included in Section 5 is the future work section.

2. LITERATURE REVIEW

Research was completed by reviewing various archival papers concerning current hybrid research and design considerations. A particular emphasis was placed on modeling the ultra-capacitors and batteries. Also of great concern was the design of a BDC motor load that would produce results that could be expected of a motor that would be applicable to an electric drive vehicle. The power electronic interface was also considered one of the primary parts of the system both in hybrid performance and overall efficiency of the system.

2.1 OVERVIEW OF HYBRID VEHICLES

Hybrid electric vehicle (HEV) systems can be composed of any number of different components or configuration types. Those typically considered involve some electrical system components and, of course, a mechanical system is required to propel the vehicle. Types of component configurations (either parallel, series, power split, or complex) in hybrids and the types of components considered such as IC engines, ultra-capacitors, batteries, or fuel cells were reviewed in [6,7]. Also covered in these papers were considerations for the type of vehicle used and the power available to the load. It was determined from these papers that the series hybrid configuration is desirable due to the ease of connecting additional electrical motors to the system if it becomes necessary.

Concerning the use of hybrids by consumers and the types of systems used, Reference [8] was a valuable resource concerning specific systems developed by car manufacturers. It was determined that there does not seem to be a standard concerning

hybrid system layout (series, parallel), voltage levels, or types of batteries used. The types of vehicles (Battery EVs, Hybrid EVs, and Fuel Cell EVs) were also discussed revealing that the most practical vehicle for modeling purposes would be the Hybrid EVs due to large amounts of prior research, which would exclude Fuel Cells, and no need for long term charging, which would exclude electric cars. Many successful hybrid manufacturers also use a permanent magnet brushless motor, with other manufacturers using either DC or induction motors.

2.2 ULTRA-CAPACITORS AND BATTERIES

Maxwell's website [1] has tools for sizing the ultra-capacitor based on desired performance characteristics and it also provides information regarding what can be expected in terms of voltage levels based on output currents and the size of the capacitor or capacitor module chosen.

References [9,10] address applications of an ultra-capacitor in an electric vehicle, while [10] also compares the ultra-capacitor to modern batteries mostly in terms of efficiency. Reference [10] also presents information comparing the power densities of ultra-capacitors and batteries. There are many different types of batteries and different approximate value models for those batteries. While some batteries are more efficient than others, as seen in Figure 2.1, the overall consideration of batteries is based on their energy density. The lead-acid battery was chosen as the battery supply considered for the series hybrid of this thesis. Of all the models, the one presented in Reference [11] seemed to present a relatively accurate model based on lead-acid battery open circuit voltage. This model takes into account the changing parameters of the battery as it is

charged and discharged. It uses a least squares approximation to determine the capacitance and resistance values during battery charging and discharging. Other battery models were considered such as that shown in Reference [12] for a Ni-MH battery model, however the model presented in [11] was chosen for its simplicity.

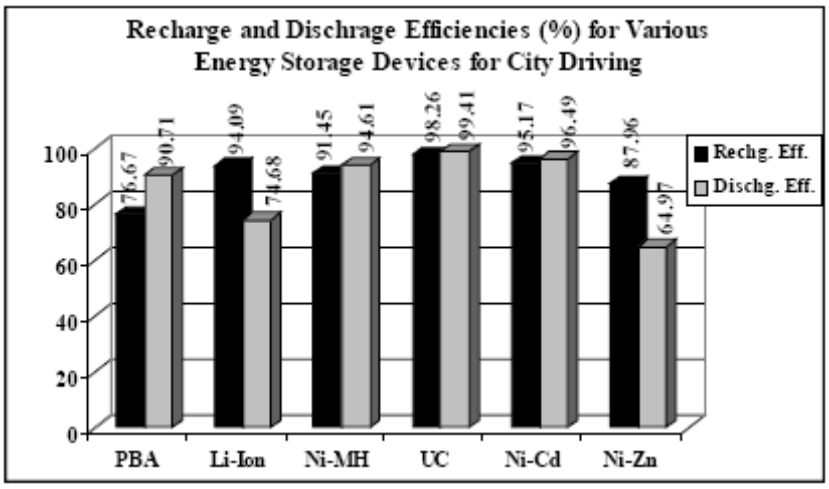

Figure 2.1. Battery and ultra-capacitor efficiencies [10]

2.3 BRUSHLESS DC MOTOR

The motor selected for the propulsion of the hybrid vehicle was selected as a brushless DC motor which has a preset model listed in MATLAB [13] which is comparable to what would be used in a hybrid electric vehicle. This model can be operated in motoring or generating mode and can be controlled via a power electronic interface. The control scheme chosen was similar to that in Reference [14] which uses

hysteresis current control to control *qdo* axis currents. Other work concerning BDC use in the vehicle design were found in References [3,6].

The generator was also considered as a permanent-magnet generator described in [15]. As discussed in this paper, permanent-magnet generators are the most likely to be used in the hybrid electric vehicle application. While this thesis focuses on design of the generator, it still offers insight as to why a PM generator should be used with an internal combustion engine as a hybrid system power source.

2.4 BI-DIRECTIONAL CONVERTER

There are many possible converters for connecting input voltages to the dc bus of the proposed hybrid. The most straight-forward design of the input DC-DC converter can be found in [5,16]. These converters have the ability to connect the power sources to the dc bus and operate in either boost or buck mode depending on whether the power source is charging the dc bus or if the dc bus is charging the power source, respectively. The output voltages are dependent on the duty cycles of each converter and can be determined based on the rated input voltages of the power source and the rated dc supply bus.

3. HYBRID SYSTEM MODELS

3.1 POWER INPUTS

3.1.1 Ultra-Capacitor Model and Characteristics. The ultra-capacitor model considered is based on the Maxwell web-site information page [1]. The Ultra-capacitor considered, BMOD0063-125V, was designed for regenerative breaking and has the characteristics shown in Figure 3.1.

Item	Performance	
Nominal Operating voltage [Vdc]	125V	
Maximum Operating Voltage [Vdc]	135V	
Surge voltage [Vdc]	142V	
Nominal Capacitance [F]	63F	
Tolerance Capacitance [%]	+20% / -0%	
DC Series resistance [mΩ]	17.0	RT
Energy Available (Whr)	101.7	Energy Available equals 1/2C (Vnom^2 – 1/2Vnom^2) /3600
Self discharge [%of initial V]	70%	30 days RT 100V; 12 hours charge and hold
Maximum Continuous Current [A]	150A	Assuming 10 degree temperature rise above ambient temperature
Max current [A]	750A	(in 5 s discharge to half nominal voltage)
Lifetime 125V, RT [hours]	150,000	End of life characterized as -20% C from nominal C, or increase of 100% in ESR
Cycles 125 to 62.5 Vdc, RT [cycles]	1,000,000	End of life characterized as -20% C from nominal C, or increase of 100% in ESR
Isolation Voltage [Vdc]	4000V	Maximum string operating voltage 1500V DC

Figure 3.1. Ultra-capacitor ratings [2]

The model used in Matlab simulations consists of a large capacitance of 63 F with a dc resistance in series of 17 mΩ. The model is shown in Figure 3.2. When modeled in Matlab, it can be seen from Figure 3.3 that this model gives a good approximation of the performance of this module during constant current discharge. The model was set for rated voltage of 50 V. For different current discharges, Figure 3.3 shows the voltage profile of the ultra-capacitor for discharge currents of 100 A and 150 A.

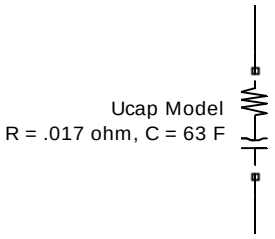

Figure 3.2. Ultra-capacitor model

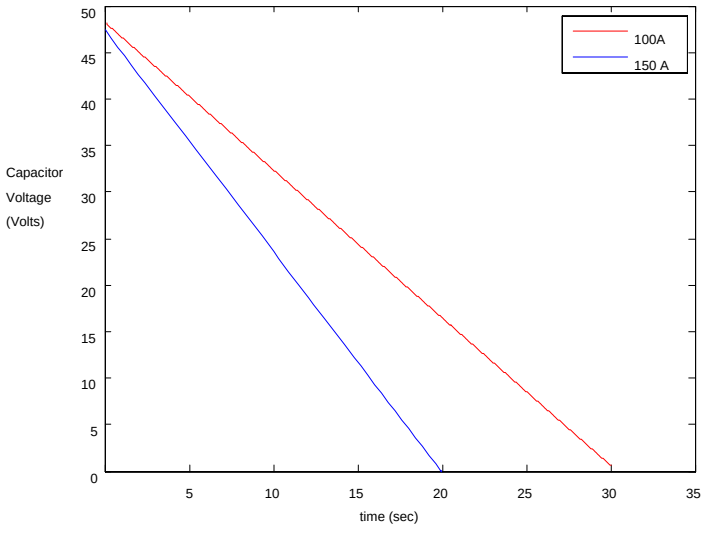

Figure 3.3. Constant current discharge of ultra-capacitor

3.1.2 Considered Battery Model and Battery Charger. The battery model in Figure 3.4 was adopted from [11]. Its defining characteristics are that the circuit parameters vary with open circuit voltage.

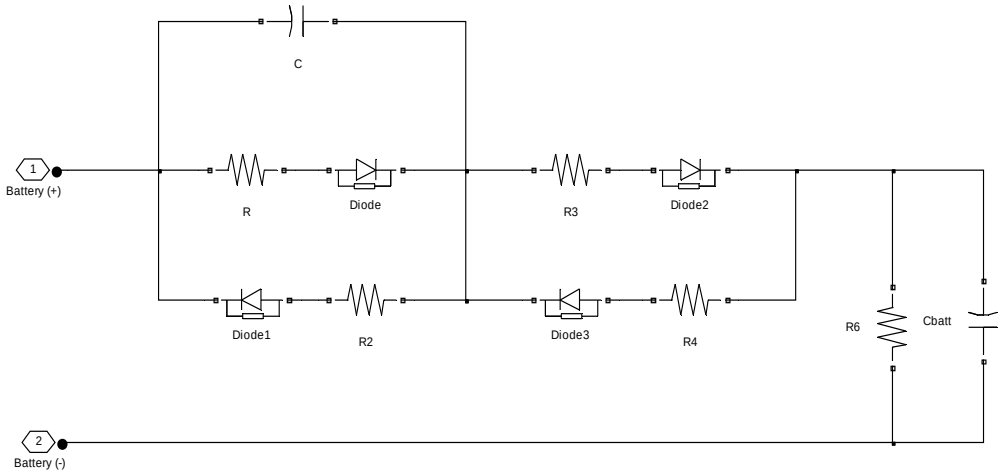

Figure 3.4. Battery model [11]

The circuit model of the lead-acid battery shows that, for charging and discharging, the circuit has different resistance values. All of the resistance and capacitance values shown in Figure 3.4 vary with open circuit voltage. The equation for any element in the model is given by:

$$Element = k \cdot e^{(wf\,(Vm-Voc))^{ff}} \tag{3.1}$$

where k is the gain, wf is the width factor, Vm is the nominal voltage, Voc is the open circuit voltage, and ff is the flatness factor. The nominal voltage is known for a battery. The gain, width factor, and flatness factor are chosen for each individual element to give charging and discharging curves for the battery that match either

manufacturer's specifications or lab tests. Figure 3.5 is the Matlab implementation of this model.

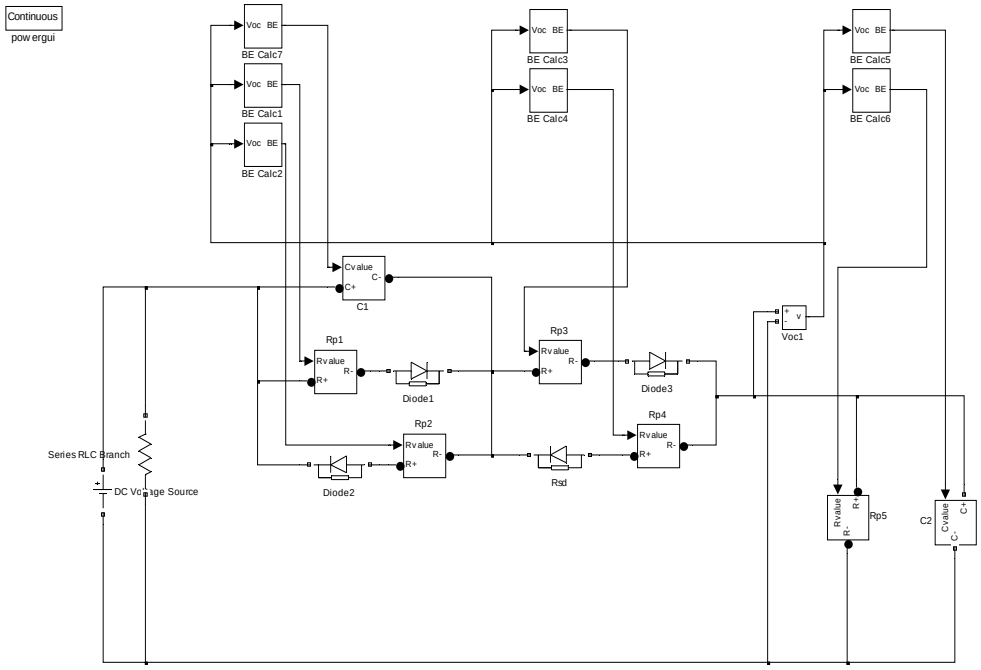

Figure 3.5. Battery model – Simulink implementation [11]

Since Matlab SimpowerSystems does not have variable resistors and variable capacitors available, these two devices were derived using controlled voltage and controlled current sources. The resistor is modeled in Figure 3.6 using The Ohm's law. The variable capacitor was modeled as shown in Figure 3.7 from

$$v(t) = \frac{1}{C}\int i(t)dt \tag{3.2}$$

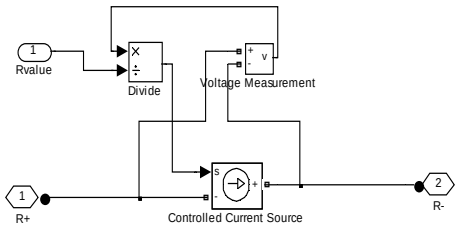

Figure 3.6. Varistor - battery model

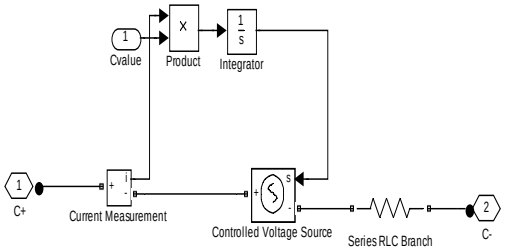

Figure 3.7. Variable capacitor - battery model

With a constant voltage source applied to the terminals of the battery, the non-linear charging performance over a period of 8 hours can be observed in Figure 3.8.

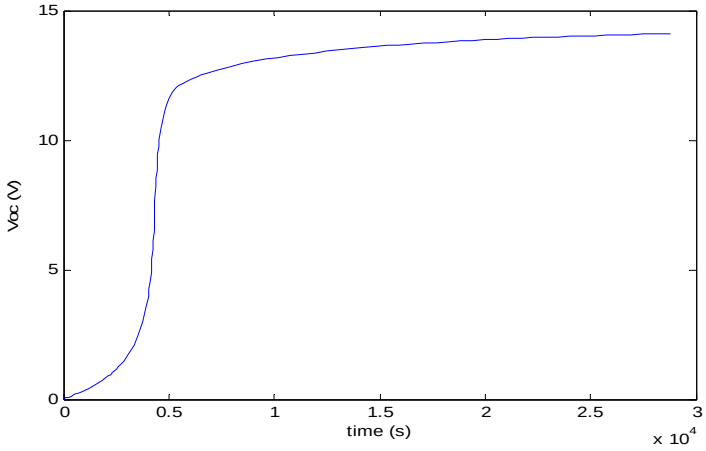

Figure 3.8. Constant voltage charge of battery

Charging of batteries for optimal performance typically involves constant current charge until the battery voltage is approximately 90% of the rated voltage. After this voltage level is reached, the charger switches to a constant voltage applied to the battery terminals. Lead acid-batteries should be kept near rated voltage or 100% state of charge (SOC) when being stored, and depending on the battery type, should be only discharged to around 90% SOC.

A battery charger model was developed as a buck converter. The battery input charging current is controlled with a PI controller to deliver constant current from a dc source larger than the rated battery voltage. After reaching approximately 90% SOC, the charger should switch to constant voltage charging. The charger model presented in this thesis is shown in Figure 3.9. The basic control scheme is to use a supply voltage of slightly more than the rated battery voltage. During constant current charging, a PI controlled duty cycle is applied to a buck converter to control charger output current. After the battery voltage reaches the desired cut-off, the buck power electronic switch is always on to provide constant voltage charging to the battery. A test for verification is done by observing the voltage and current waveforms when applied to a parallel RC load. Assuming this particular "battery" is rated at 12.5 V, the dc input voltage to the charger is 13.5 V. A resistance of 1 MΩ and a capacitance of 40 F were used for the test. It can be seen in Figures 3.10 and 3.11 that the charger brings the charging current to the demanded value of 10 A. After the nominal voltage is reached, the duty cycle of the converter is set to 1 for constant voltage charge.

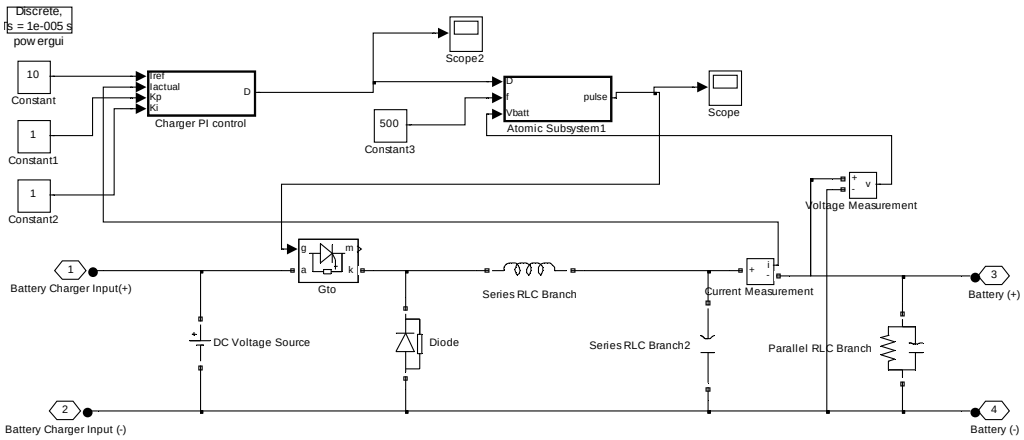

Figure 3.9. Battery charger model

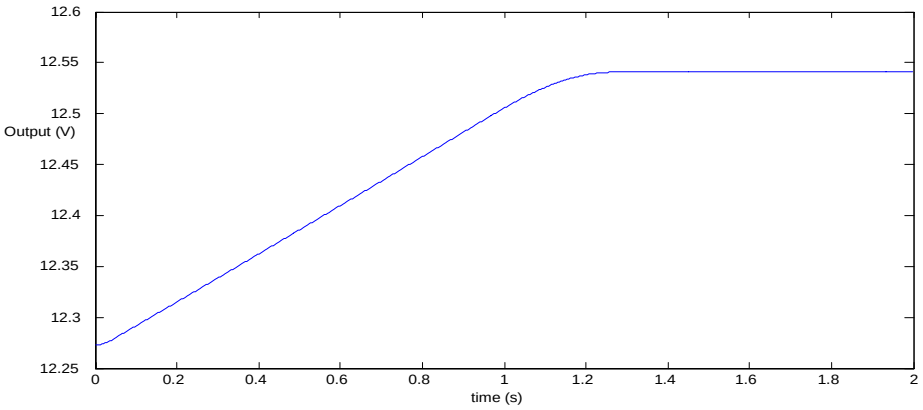

Figure 3.10 Charger output voltage

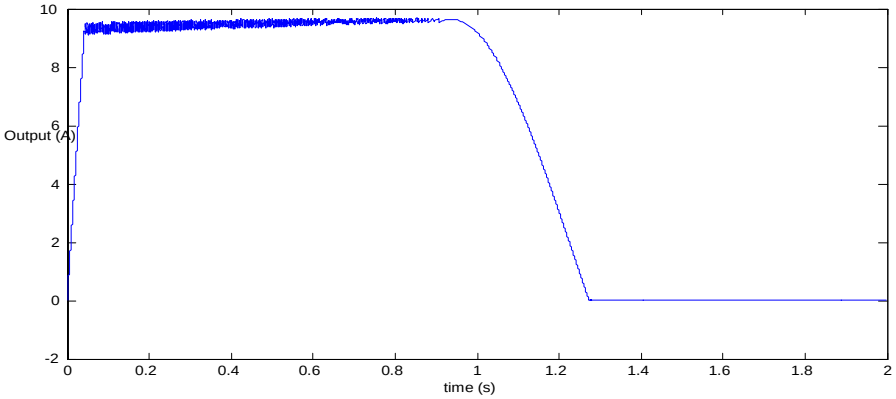

Figure 3.11 Charger output current

With the battery model and battery charger designed, it may be possible to verify the battery model's characteristics by comparing them to the manufacturer's data. Unfortunately, the non-linear battery model only operates well in Matlab under continuous simulation mode. The charger only operates well in discrete power GUI mode and would take days to simulate over the 8-hr. charging period of a normal lead-acid battery in order to verify battery specifications. Because of this simulation performance problem encountered, it was decided to leave out the battery model included in the original hybrid mainly because the battery model could not be verified through simulations to approximate any battery model described in manufacturer's specifications.

3.1.3 Generator Model. The generator model consists of a PMSM with a controlled mechanical input speed. The PMSM generator has the same ratings as the BDC motor and is designed to ramp up to the rated speed if needed. The output voltage of the three phase generator is then rectified to deliver a dc voltage source. The attractive features of the PMSM as a generator are high torque per volume, high efficiency, and compactness [15]. Figure 3.12 illustrates the proposed model of the PMSM generator and the three phase rectifier. It can be seen in Figure 3.13 that, at rated speed with a $1\,\Omega$ resistive load and a $10\,\mathrm{k}\Omega$ resistive load, the output voltage of the generator is typically near the value of 150 V to 250 V depending on the amount of current demanded by the load.

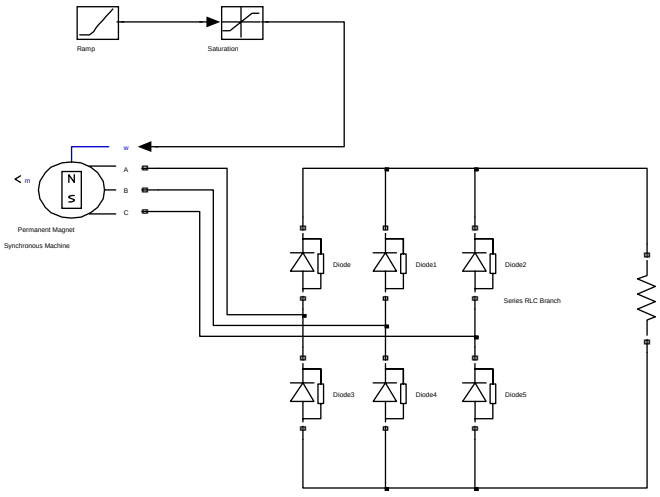

Figure 3.12. Generator model

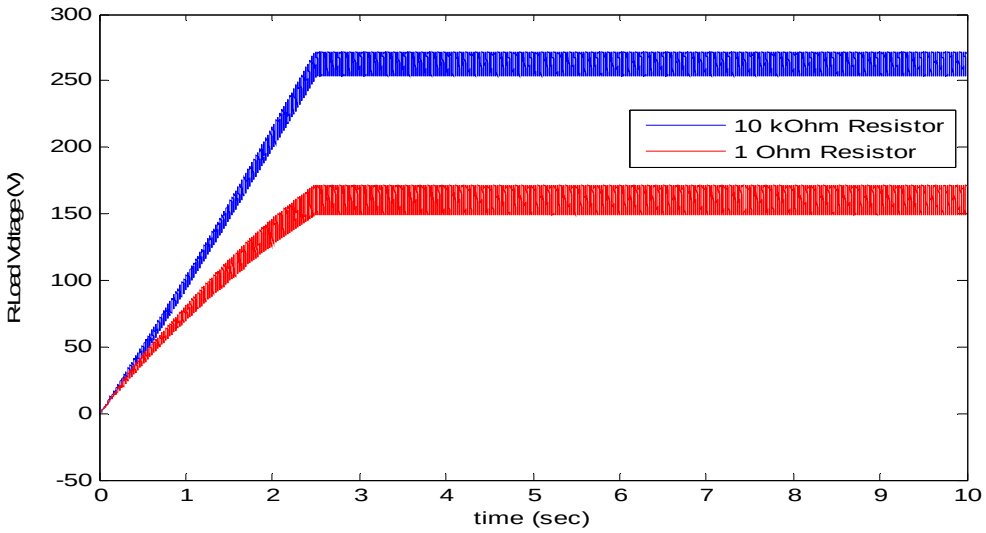

Figure 3.13. Generator output voltage

Figure 3.14 shows the output power for different speeds; the output power of the generator to the load is dependent on the mechanical rotor speed of the PMSM. At rated speed, the power delivered to the load is the rated power of the PMSM of

26.3 kW. The bands in the outputs of Figures 3.13 and 3.14 are due to the rectification of sinusoidal waveforms.

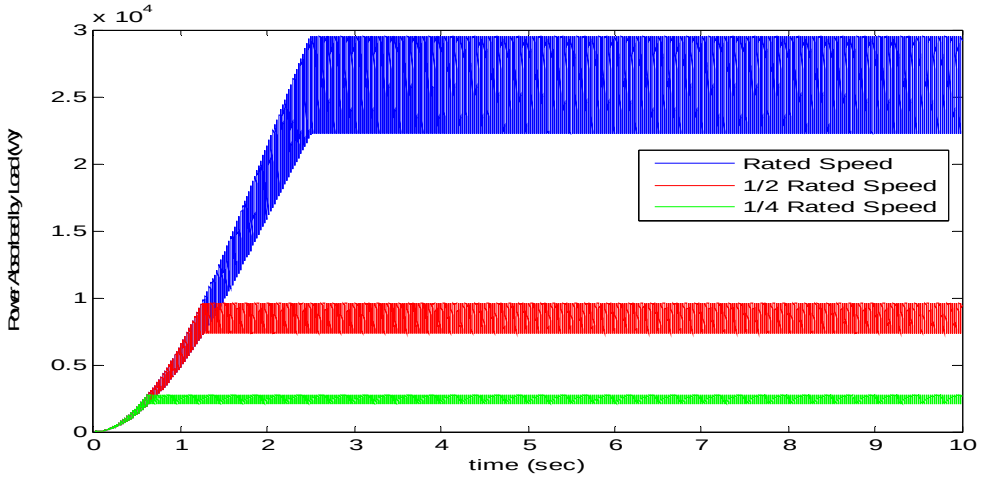

Figure 3.14. Generator output power for a $1\,\Omega$ load

This generator is to be coupled with a speed controlled IC engine which will provide the power at the input of the generator in an actual vehicle. Control of the PMSM generator is illustrated in Figure 3.15. The control diagram and proposed overall control of the PMSM generator is shown in Figure 3.15(a). The generator is the primary source of power in the system and is used to provide power to the main dc bus whenever there is a long duration sag in voltage.

In the simulation the mechanical speed of the PMSM generator is controlled by PI controller, and because mechanically the rotor speed can not go from 0 rad/s to rated speed of 314 rad/sec, the output of the ω value, corresponding to the mechanical rotor speed, is both limited in terms of speed and acceleration all within

the PI controller. The Matlab model for the PI controller is shown in Figure 3.15(b). The logic for the PI control is:

- when dc bus voltage is less than 400 V: set-point output voltage of rectified generator voltage is 200 V
- when dc bus voltage is greater than 400 V: set-point output voltage of rectified generator voltage is 0 V

Math model equations for PI control are

$$\omega = error * (K_P + \frac{K_I}{s})$$

Error is the difference between the set-point and actual voltage of the rectified generator output. K_P is the proportional gain and K_I is the integral gain. $\frac{1}{s}$ is the integral, and ω is rated limited and maximum value limited. Whenever the dc bus voltage of the system drops below the value of 400 V, the generator is turned on and used in conjunction with a boost converter, at the output of the generator dc terminals, to supply power to the dc voltage bus.

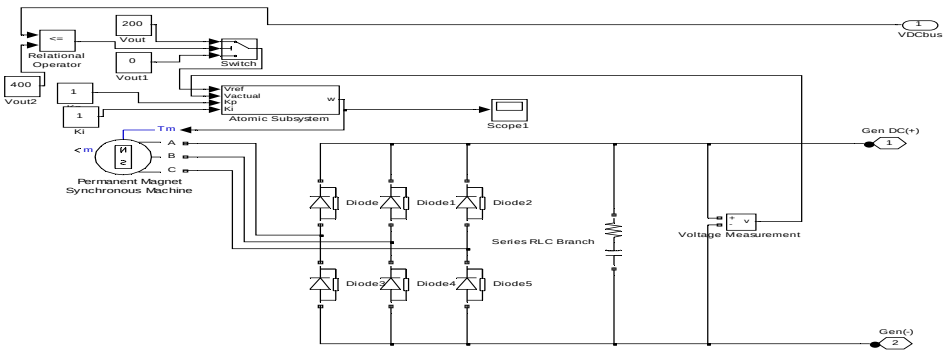

(a) PMSM generator control

Figure 3.15. Generator

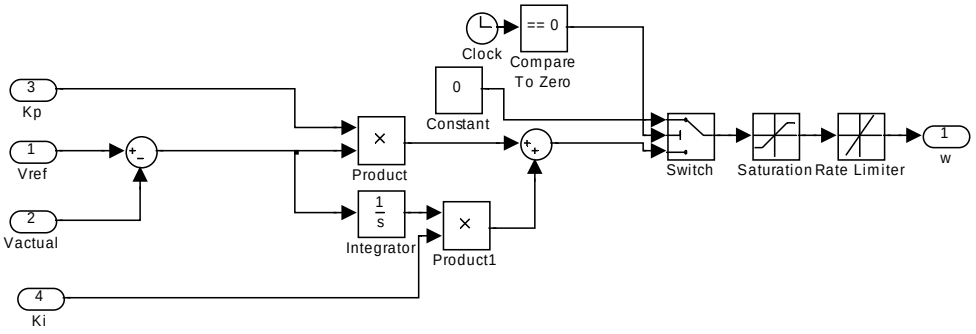

(b) Rate limited PI control of generator rotor speed
Figure 3.15. Generator (cont.)

To simplify the controls and make the system more stable, the duty-cycle of the boost converter is a set value of 0.1 to limit current as shown in Figure 3.16(a). The boost converter is located between the dc output of the generator and the dc bus. The gate pulse into the converter is shown in Figure 3.16(b). This pulse is dependent on duty cycle and switching frequency. For a duty cycle of .1 and a switching frequency of 5kHz, the pulse output is shown to be accurate in Figure 3.16(b).

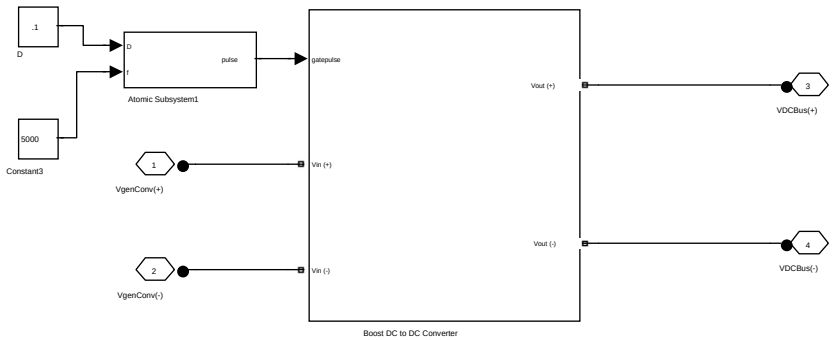

(a) Fixed generator boost converter duty cycle –
Figure 3.16. Converter

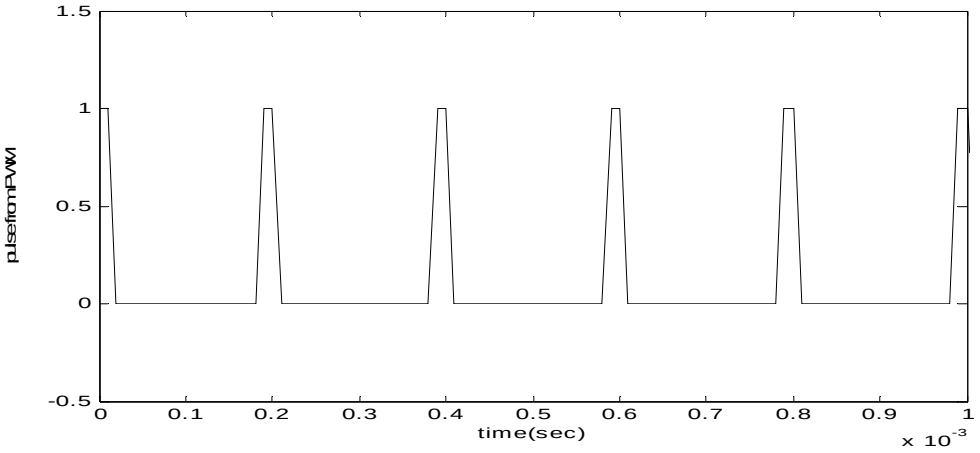

(b) Pulse to converter
Figure 3.16. Converter (cont.)

Figure 3.17 is the design of the boost converter for charging the dc bus. The output voltage is dependent on the input voltage and the duty cycle of the converter. The overall purpose of the generator is to supply most of the necessary power of the hybrid vehicle in terms of motor power supply and in recharging the ultra-capacitors in the system.

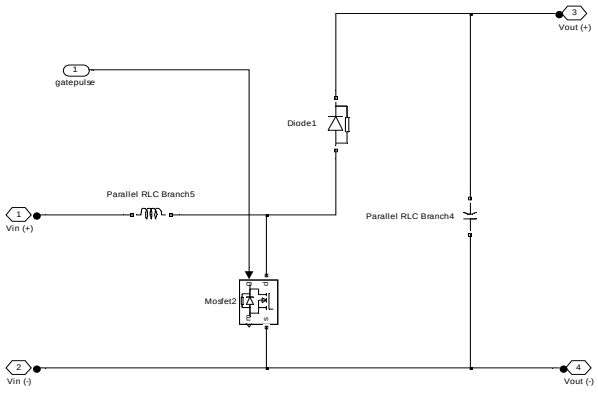

Figure 3.17. Generator boost converter

3.2 SYSTEM LOAD

The proposed system motor is a Brushless DC machine. Because SimPowersystems was the chosen software for simulation of the system, it was decided to take advantage of the available machine models in this software toolbox. The main area of difficulty is then operating the machine to get optimal performance out of the system by using a power electronic interface.

A BDC motor was chosen for vehicle propulsion because it has high efficiency and it is relatively easy to control if the rotor position and speed are known. The control strategy of hysteresis current control was chosen due to its sensitivity to dc bus voltage, which appears to be an issue among some commercially available DC drives.

Because many power drive systems seem to be very sensitive to dc voltage supply levels, a hysteresis control model was selected similar to what was developed in [14] because it is capable of supplying the needed torque to the BDC model, but it is also very sensitive to dc voltage supply. The model of the hysteresis current controlled system is presented with controlled MOSFETs based on desired mechanical speeds of the BDC motor. The assumptions are that the rotor position and the speed are both known accurately for this control method.

The proposed Brushless DC motor has the characteristics listed in Table 3.1. The overall system layout of the BDC driver and BDC motor is shown in Figure 3.18. This layout consists of a MOSFET universal bridge, BDC motor, PI controller, and a hysteresis current controller.

Table 3.1 BDC Machine Characteristics [13]

Parameter	Rating
Torque	42.09 N*m
Max DC Input Voltage	560
Speed Rating	3000 RPM, 314.16 rad/sec
Stator Resitance	0.0485 ohms
Magnet Flux Induced	0.1194 Wb
Moment of Interia	0.0027 kg*m2
Frictional Force	0.0004924 N*m*s
Poles	4

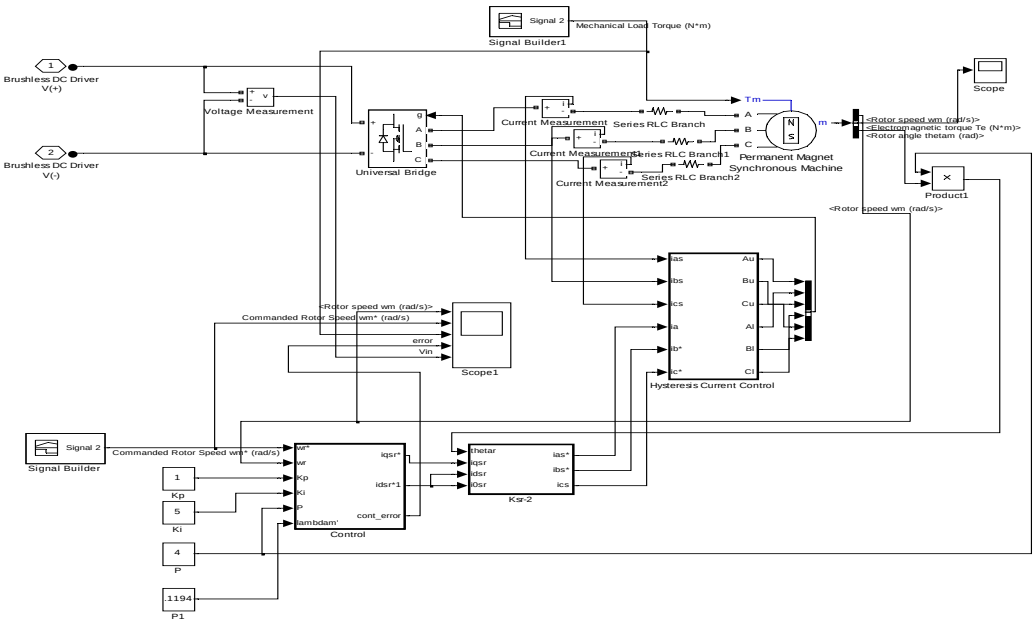

Figure 3.18. BDC motor control

Brushless DC voltage equations from [13,14] are as follows assuming a sinusoidal back emf, electro-motive force, for the motor:

$$\begin{aligned} v_{as} &= r_s i_{as} + L_{ss}\frac{di_{as}}{dt} + \omega_r \lambda_m^{'} \cos(\theta_r) \\ v_{bs} &= r_s i_{bs} + L_{ss}\frac{di_{bs}}{dt} + \omega_r \lambda_m^{'} \cos(\theta_r - \frac{2\pi}{3}) \\ v_{cs} &= r_s i_{cs} + L_{ss}\frac{di_{cs}}{dt} + \omega_r \lambda_m^{'} \cos(\theta_r + \frac{2\pi}{3}) \end{aligned} \tag{3.3}$$

Where r_s is the stator resistance, ω_r is the electrical rotor speed, and $\lambda_m^{'}$ is the flux induced by the magnets. From equations derived in [14] the following calculations were made to determine necessary control information for the Matlab Brushless DC motor. Using rotor position, θ_m, the electrical rotor position, θ_r, can be determined from:

$$\theta_r = \frac{P}{2} \cdot \theta_m \tag{3.4}$$

Where P represents the number of poles of the BDC motor. The electrical angle of the machine can then be used to convert between the *qd0*-axis reference frame variables and abc variables using the transformation matrices. The transformations from *abc* to the *qdo* reference frame equation given by:

$$f_{qd0s}^{r} = K_s^r \cdot f_{abcs} \tag{3.5}$$

Transformations from *qd0* axis variables to the abc values are given by:

$$f_{abcs} = K_s^{r-1} \cdot f_{qd0s}^{r} \tag{3.6}$$

Where f represents the converted value (current, voltage, etc.) and

$$K_s^r = \frac{2}{3}\begin{pmatrix} \cos(\theta_r) & \cos(\theta_r - \frac{2\pi}{3}) & \cos(\theta_r + \frac{2\pi}{3}) \\ \sin(\theta_r) & \sin(\theta_r - \frac{2\pi}{3}) & \sin(\theta_r + \frac{2\pi}{3}) \\ \frac{1}{2} & \frac{1}{2} & \frac{1}{2} \end{pmatrix} \tag{3.7}$$

And

$$K_s^{r-1} = \begin{pmatrix} \cos(\theta_r) & \sin(\theta_r) & 1 \\ \cos(\theta_r - \frac{2\pi}{3}) & \sin(\theta_r - \frac{2\pi}{3}) & 1 \\ \cos(\theta_r + \frac{2\pi}{3}) & \sin(\theta_r + \frac{2\pi}{3}) & 1 \end{pmatrix} \tag{3.8}$$

These transformation matrices can be used to determine voltages and currents in the system for easier control. These transformations will allow for speed control of the system. Also from [14] the commanded torque can be referenced in the qd0 reference frame by the equation

$$T_e = \frac{3}{2} * \frac{P}{2} * i_{qs}^r \tag{3.9}$$

The desired value of electrical torque is necessary for determining the needed q-axis current for optimal performance of the BDC drive.

Using rotor mechanical position and rotor mechanical speed along with referencing variables between the two different reference frames with equation (3.8), the torque of the motor is controlled via error readings between the commanded rotor mechanical speed and the actual rotor mechanical speed. This error is then sent to a

PI controller, in Figure 3.18, that determines the torque and the q-axis current needed for error correction.

The hysteresis control operates similar to that of what was discussed in [14]. After the commanded q-axis current is determined, the *abc* commanded currents are calculated using equation (3.8). If the commanded phase current is greater than the actual current plus the hysteresis band, then the upper switch of that phase is turned off and the lower switch of that phase is turned on to lower phase current. If the commanded phase current is lower than the commanded current minus the hysteresis band, the upper switch of the inverter is turned on and the lower switch is turned off to increase phase current.

The three-phase, six-switch inverter is used as the power electronic interface. It is composed of six power electronic switches, two switches per phase, to control input currents to the BDC motor. The switches used are power MOSFETs. With an input voltage of 400 V to the BDC driver, the BDC motor was tested to determine performance of the motor. In Figure 3.19 the commanded motor speed is shown starting at zero, leveling off at near rated speed, going slightly negative and then returning to zero. Figure 3.20 shows that the actual rotor speed follows the commanded speed very closely during all stages of commanded rotor speed. Even during peak load and speed conditions the desired speed is delivered by the system. The applied mechanical load torque to the BDC motor is seen in Figure 3.21. The commanded torque increases gradually from zero to 13 N*m then drops off sharply before going negative. The mechanical load torque then returns to zero.

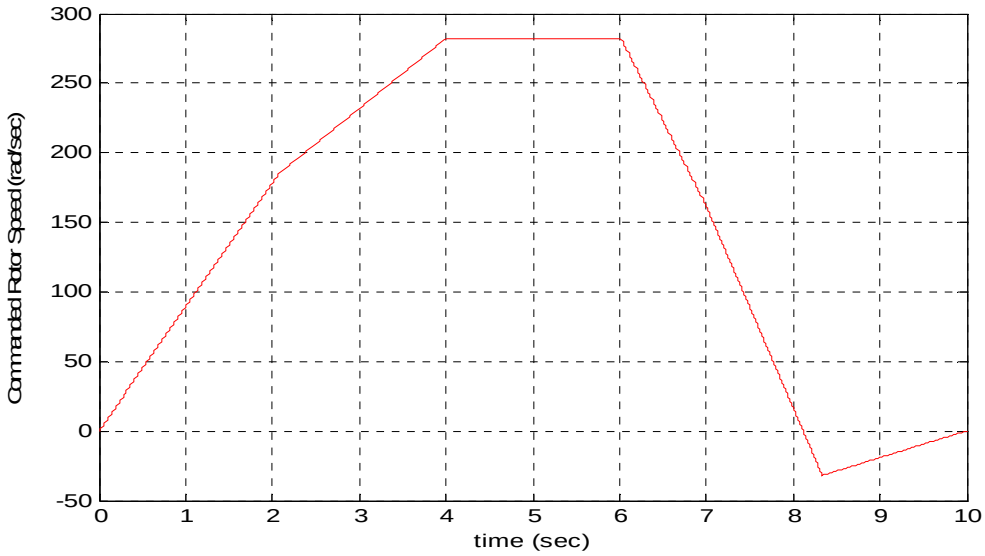

Figure 3.19. Commanded motor speed – 400 V supply

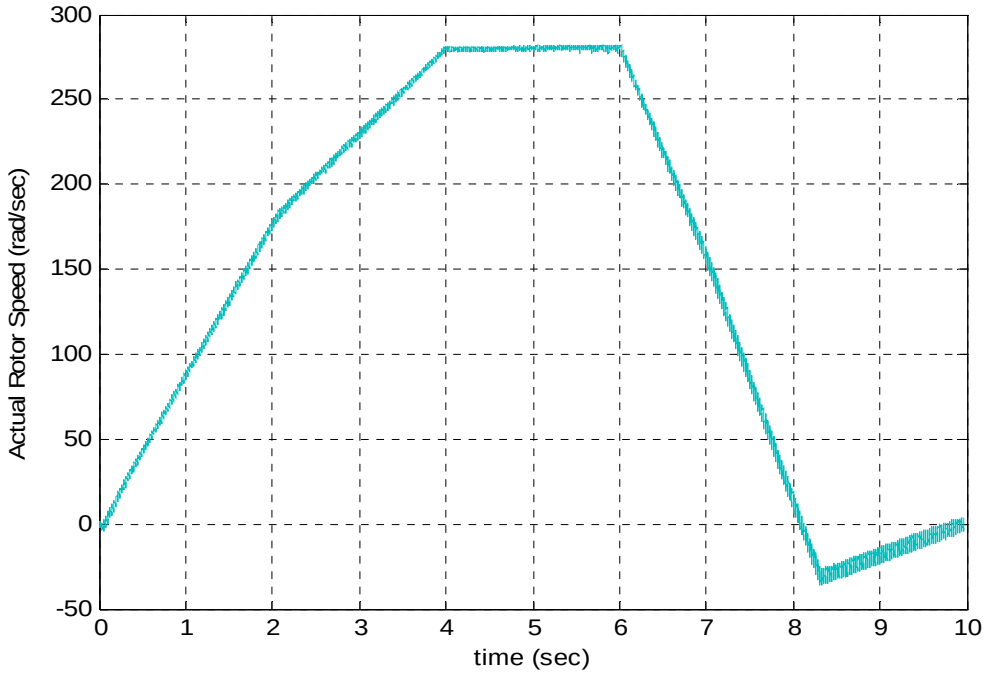

Figure 3.20. Actual motor speed – 400 V supply

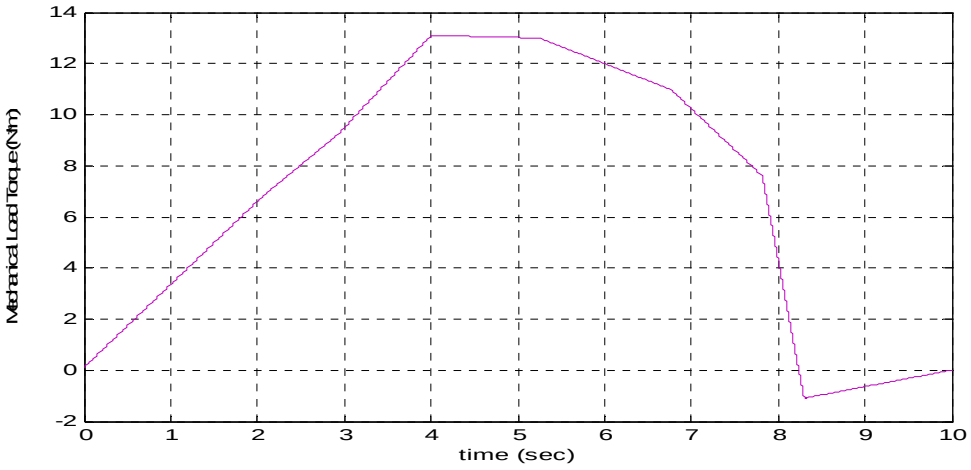

Figure 3.21. Mechanical load torque – 400 V supply

The error, or difference between commanded speed and actual speed, of the system can be seen in Figure 3.22. The small initial error is due to the mechanical torque at the beginning of the simulation. The error is kept consistently small even during peak load conditions at the simulation time of 4 sec.

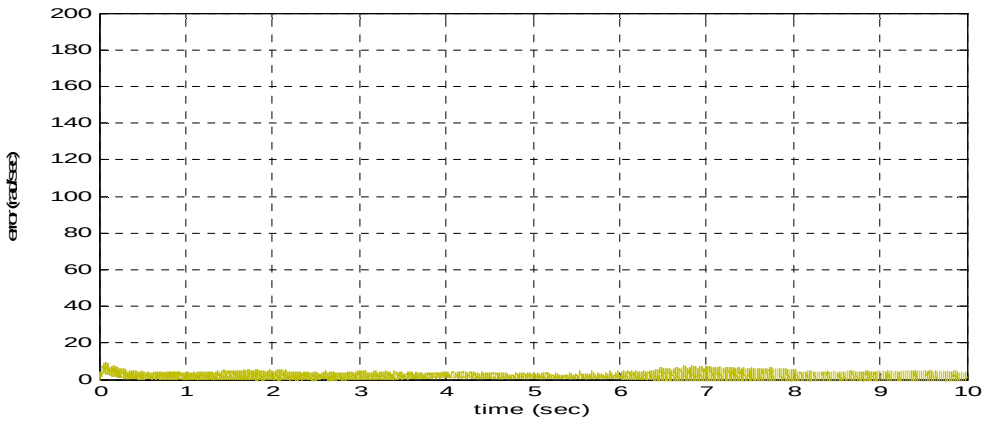

Figure 3.22. BDC speed error – 400 V supply

When the supply voltage is set to 300 V, the BDC motor encounters performance problems. Figure 3.23 shows both the commanded rotor speed and the actual rotor speed. The commanded speed and the mechanical load torque were the same as in the previous simulation.

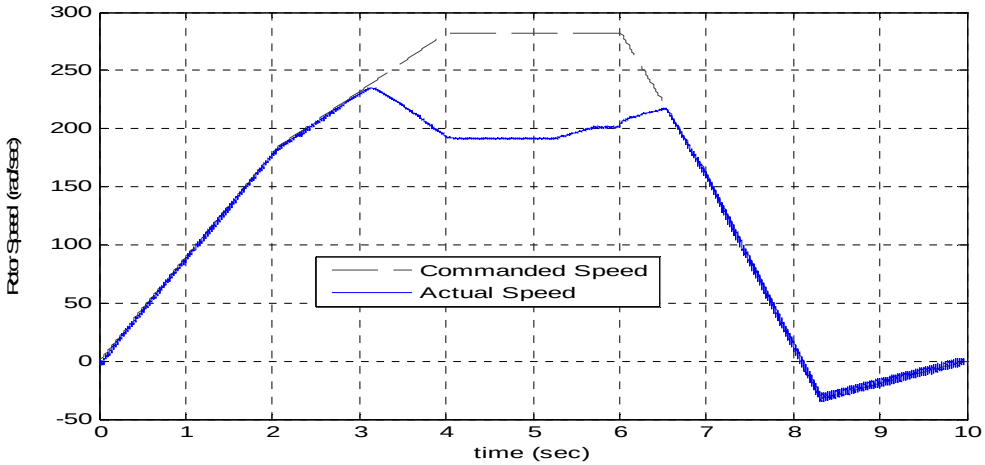

Figure 3.23. Motor speed – 300 V supply

The actual rotor speed is not able to follow the commanded rotor speed with a lower dc input voltage. This shows that a specific input voltage is necessary depending on the power requirements of the BDC motor. Figure 3.24 shows the mechanical load torque of the system. Figure 3.25 shows speed error. The error occurs when the BDC motor requires more voltage than is provided, and the peak error occurs when load torque and commanded speed are at their maximum values. The BDC motor requires a constant dc voltage supply for optimal performance. To supply this constant voltage, coordination of the generator and the ultra-capacitor is necessary.

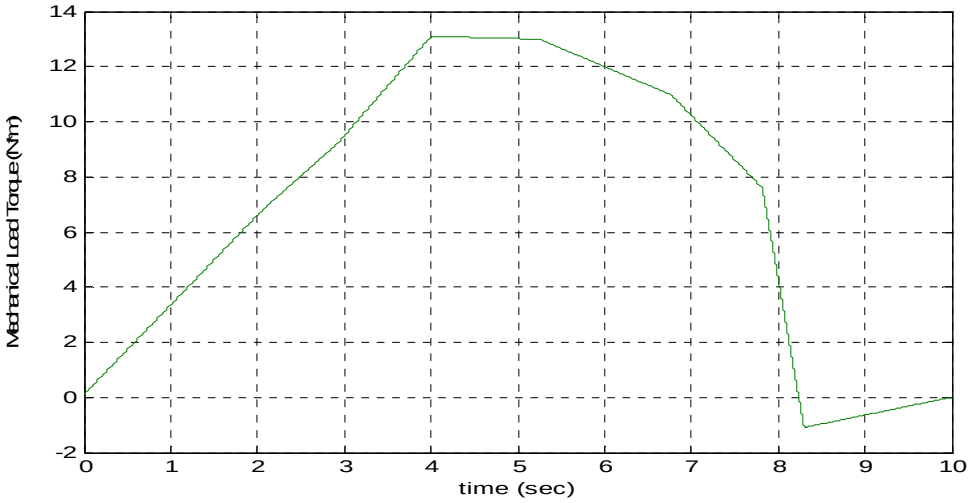

Figure 3.24 Mechanical load torque – 300 V supply

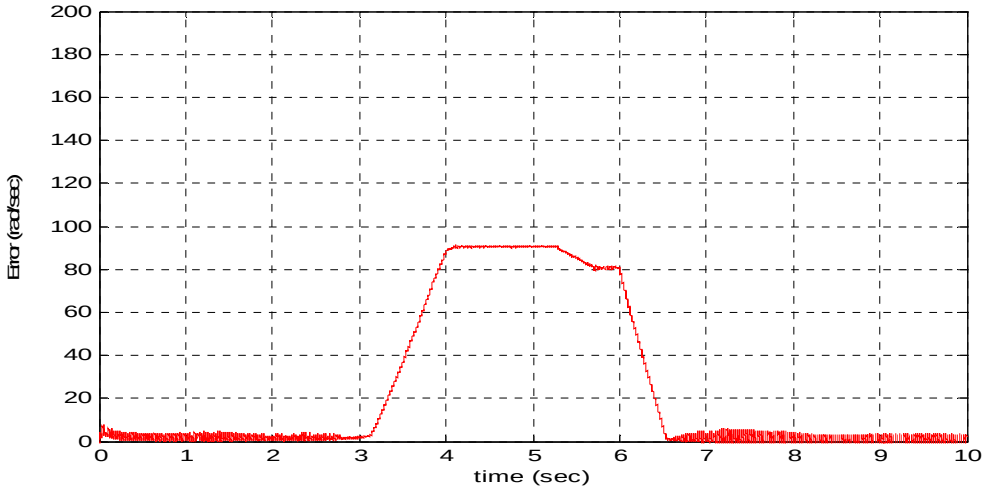

Figure 3.25 BDC speed error – 300 V supply

3.3 POWER ELECTRONIC CONTROL

Because the dc bus voltage is high, there is a necessity for power converters between the power sources that are typically rated at much lower voltages, but can nonetheless supply currents to the dc bus. The general control of the system is to

have a buck-boost converter between the ultra-capacitor and the dc bus and a boost converter between the PMSM generator and the dc bus. The buck-boost converter referenced in [5] was used to supply power between the ultra-capacitor and the dc bus. An illustration of this converter is seen in Figure 3.26. This converter operates in 3 different modes. The lower MOSFET controls the boost mode in Mode 1. In Mode 2, the upper MOSFET controls the buck mode. Mode 3 is when both switches are in the off position to effectively stop power flow.

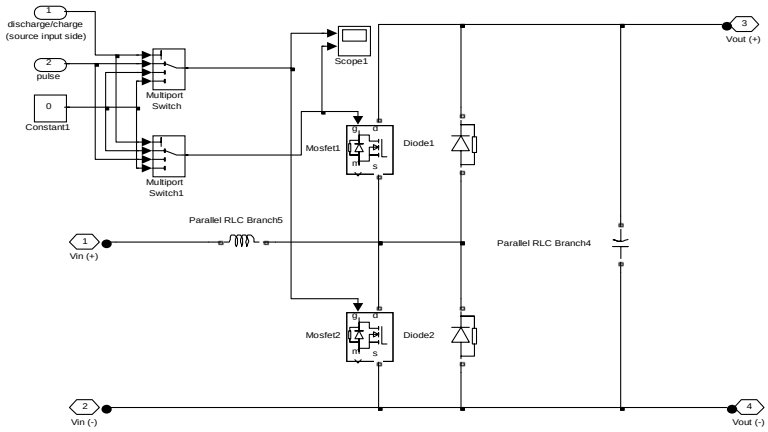

Figure 3.26. Bi-directional converter [5]

The mode of operation is dependent on the voltage of the dc bus and the voltage across the terminals of the ultra-capacitor. When there is a sag in voltage at the dc bus, the converter operates in the Boost mode to supply current to the dc bus. The duty cycle in the boost mode is limited to limit discharge currents from the ultra-capacitor. The boost operation equation for an ideal boost converter [17] concerning input and output is given as

$$V_0 = \frac{V_s}{1-D} \tag{3.10}$$

Where V_s is the supply voltage, V_o is the output voltage of the boost converter and D is the duty cycle of the power electronic switch. In the simulation, the maximum limit of D was tested to determine when the output current of the ultra-capacitor did not exceed a rated switch current of around 50 A. The current that could potentially be supplied by the UC is much larger, but due to limits on the switching speed within the simulation, the desired current input to the ultra-capacitor is set at 50 A with low switching speeds. A diagram of Boost mode operation is shown in Figure 3.27.

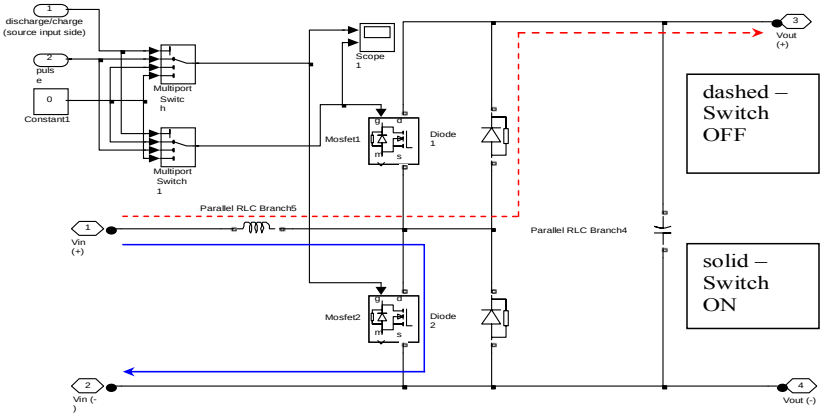

Figure 3.27. Bi-directional converter - boost mode

In the buck mode, the ultra-capacitor is then charged to the rated voltage. The output voltage equation for buck mode [17] is

$$V_o = DVs \tag{3.11}$$

It can be seen from equation (3.11) that the output voltage of the converter is dependent on the duty cycle of the MOSFET. A diagram of the converter in the buck

mode can be seen in Figure 3.28. The boost converter is similar to the bi-directional converter but with a missing MOSFET for the buck mode.

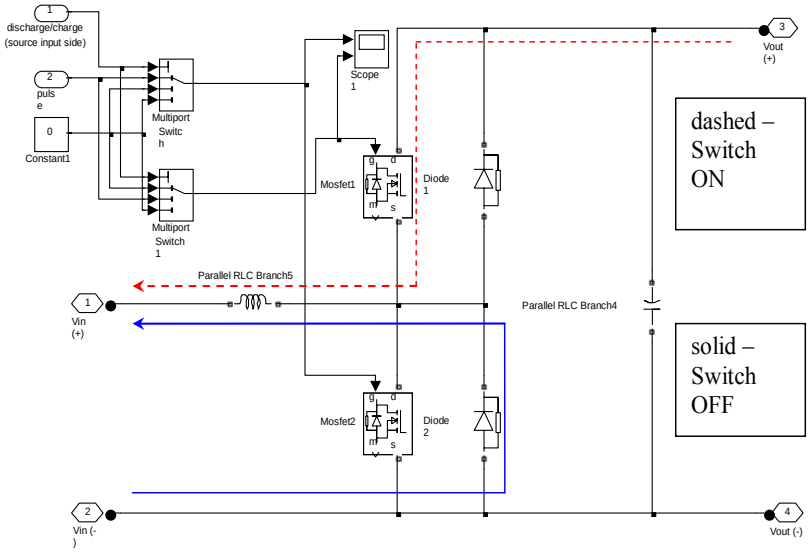

3.28. Bi-directional converter - buck mode

The control of the bi-directional DC-DC converter is illustrated in Figure 3.29. The mode of operation is determined by the voltages applied at both the terminals to the UC and the dc bus voltage. When excess voltage is read on the dc bus, the bi-directional converter can begin the buck mode (charging UC). When the dc voltage dips below the minimum dc voltage of the bus, the UC provides power with the converter operating in the boost mode. The control logic is set-up to only allow charging of the UC if the dc bus voltage exceeds the maximum dc bus voltage of 385 V. The operation of the bi-directional converter is designed so that it can provide power during quick changes in the commanded performance of the BDC

motor. It also operates in a mode that allows the ultra-capacitor to absorb some of the power involved in regenerative braking.

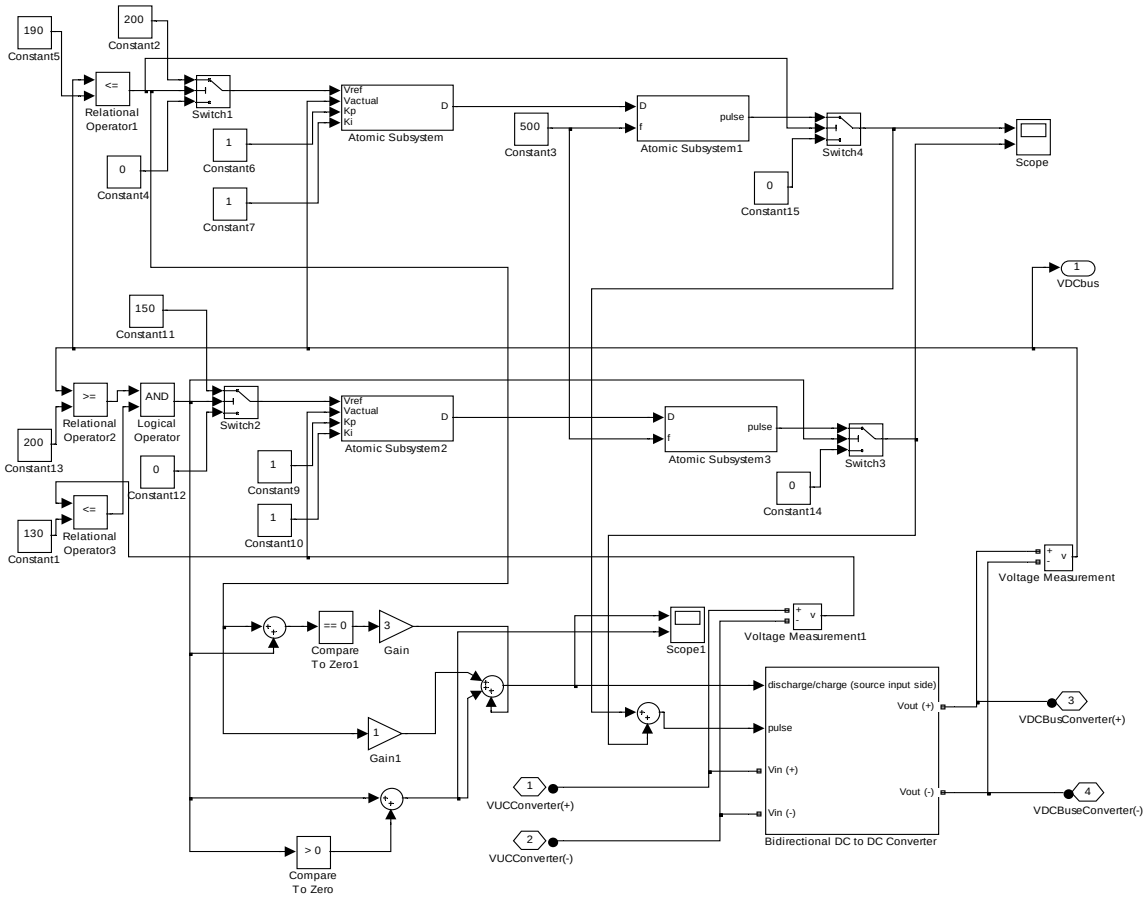

Figure 3.29 Bi-directional converter – controller

4. OVERALL SYSTEM LAYOUT AND PERFORMANCE

The complete system consists of an ultra-capacitor and a generator in a series hybrid configuration to provide power through converters to a dc bus that supplies power to a BDC propulsion motor as shown in Figure 4.1.

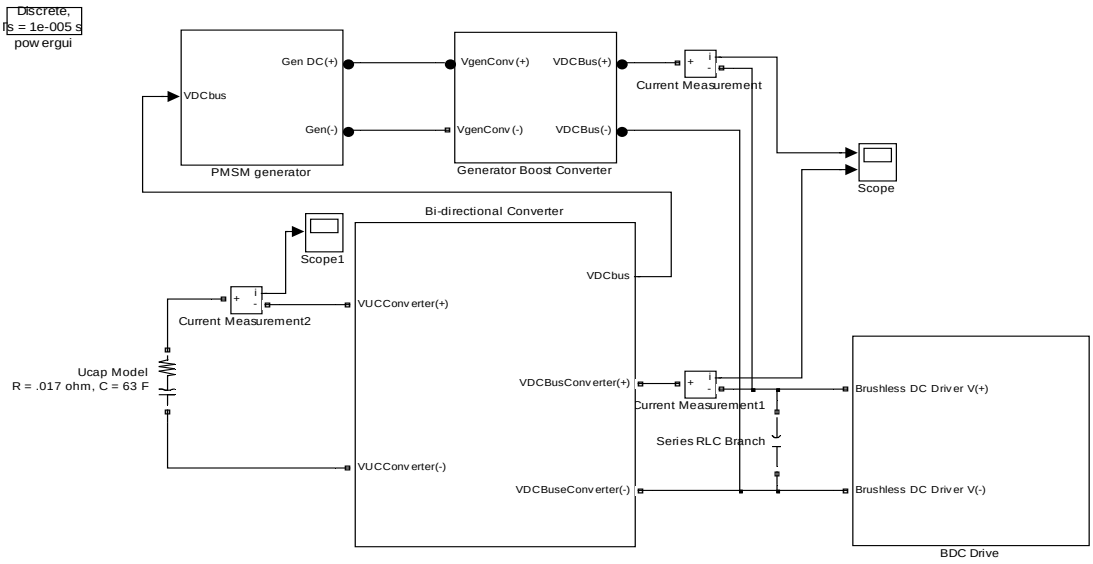

Figure 4.1. The hybrid power system layout implementation in Matlab

For data collection purposes, the performance of the BDC motor is monitored to inspect rotor speed, rotor speed error, dc supply voltage, and current injections from the two power sources. The goals are to show:

- The Ultra-Capacitor alone has difficulty supplying all of the load power due to limitations on injected currents.

- The PMSM generator can supply sufficient power to the system but initially the voltage sags as the generator speed is ramped.
- At low speeds and torques, the ultra-capacitor will support the dc bus voltage.
- At higher speeds the power from the PMSM generator is needed for better system performance.
- Regeneration occurs when the BDC motor is in generation mode and the dc bus voltage is near system rated value

The first series of tests is to confirm operation of each individual component of the system under a defined set of commanded speed and applied mechanical load for the BDC motor. Current supplied by each device should illustrate what is occurring in the system concerning how much power is supplied by each device as well as how much power the load is demanding from the power sources.

4.1 ULTRA-CAPACITOR ONLY OPERATION

When only the ultra-capacitor is used as a power supply, simulations show that at lower torque and speed demands from the BDC drive that the ultra-capacitor UC acts sufficiently to supply power to the system as seen in Figure 4.2. When the mechanical torque to the motor is applied at higher levels and more speed is requested of the BDC motor, the error starts to increase peaking at maximum commanded speed and maximum load torque. The load torque is shown in Figure 4.3. This error also corresponds to a lower than desired value of voltage at the dc supply bus of the BDC drive. The peak power supplied by the ultra-capacitor is $T \cdot \omega$, approximately $(7N \cdot m) \cdot (125 rad/\sec)$, or 875 W.

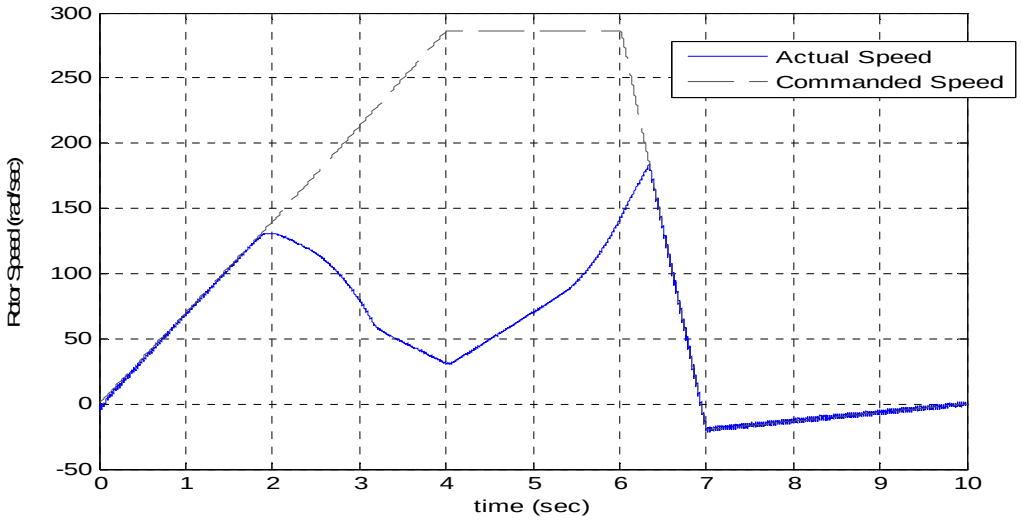

4.2. Ultra-capacitor only - rotor speed

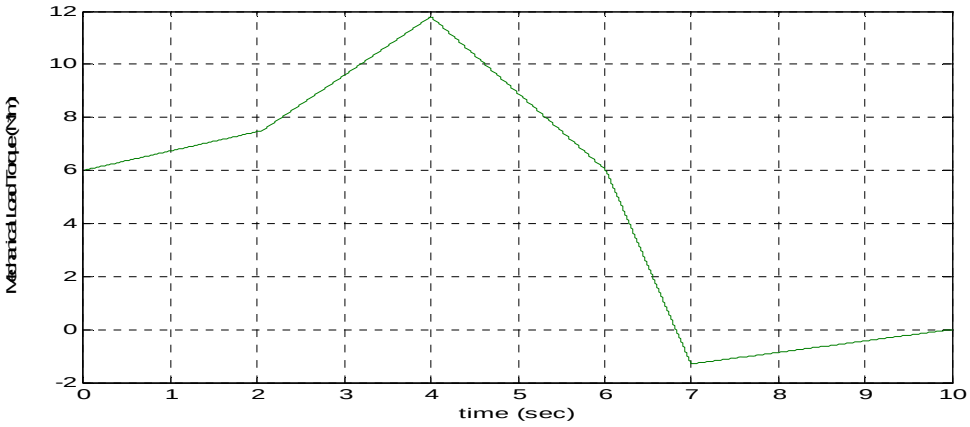

4.3. Ultra-capacitor only – mechanical load torque

Current information regarding the ultra-capacitor is shown in Figure 4. The current contribution from the ultra-capacitor is shown in Figure 4.4(a). Low pass filtering of the current contributions of the power sources is necessary to determine average currents both to and from sources. A Matlab implementation of a low pass filter is shown in Figure 4.4(b). The low-pass filtered current contribution is shown

in Figure 4.4(c). The current pulses are limited by the duty cycle of the bi-directional converter which is kept to a low value. Current values never exceed 40 A.

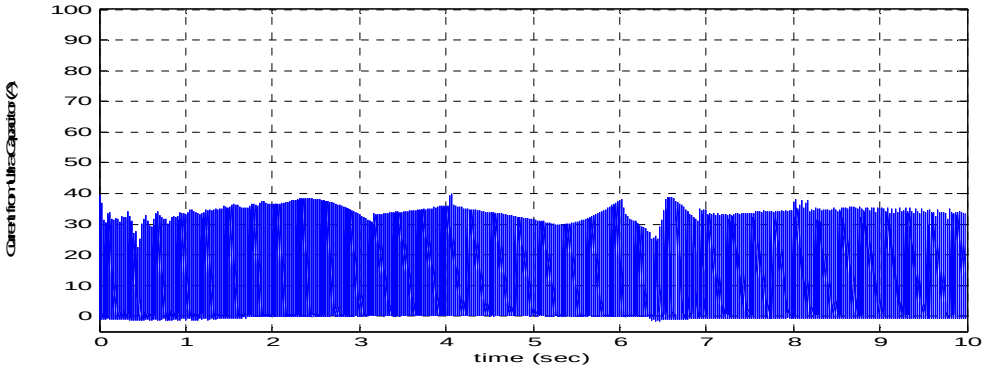

(a) Ultra- capacitor only - current contribution

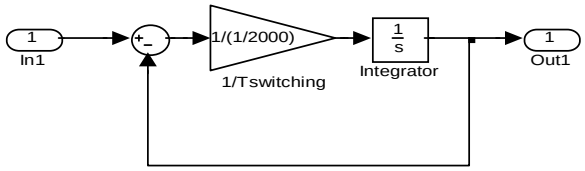

(b) Current low-pass filtering

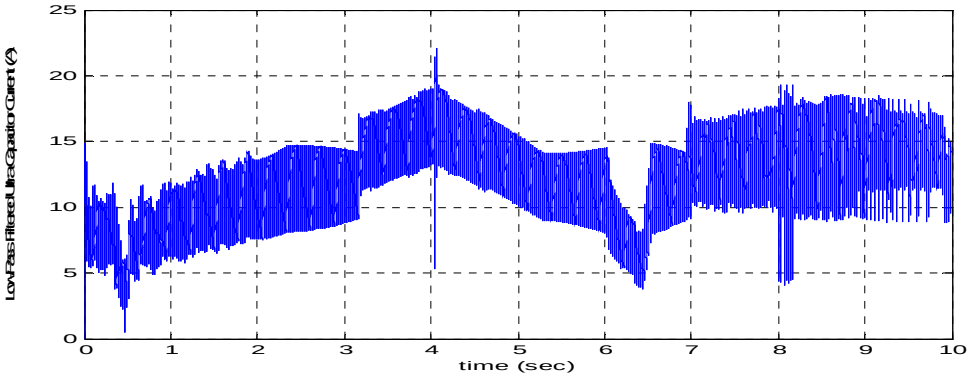

(c) Ultra-capacitor only – filtered current contribution –
Figure 4.4. Currents

Initially it is assumed that the ultra-capacitor is fully charged and the dc bus capacitor is charged to 160V. At the beginning of the simulation, the ultra-capacitor supplies a sufficient current to the dc bus capacitor to maintain a bus voltage of almost 200 V. That bus voltage remains constant until the mechanical load torque and the commanded speed increase which would require a larger dc supply voltage. In such an event, current is drained from the dc bus capacitor and the capacitor voltage begins to sag as seen in Figure 4.5.

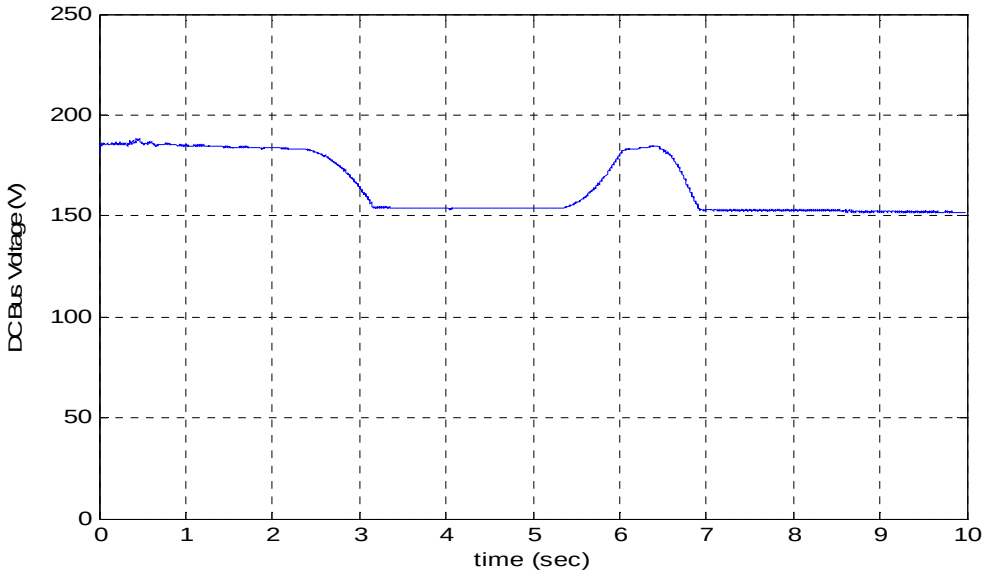

Figure 4.5. Ultra-capacitor only – dc bus voltage

4.2 GENERATOR ONLY OPERATION

The assumption is that the generator operates by a mechanically coupled IC engine that is speed controlled. The speed of the PMSM generator is proportional to the power delivered to the system. Due to this speed control, it is assumed that the

generator rotor speed has to be rate limited to make the system more realistic (i.e. generator rotor speed cannot change from 0 to the rated speed instantaneously). The maximum rotor speed is limited to rated to the mechanical speed of 314 rad/sec, and the speed change of the rotor is assumed to be from 0 rad/sec to rated speed (3000 RPM) in 2.5 sec and the rated speed to 0 rad/sec in 1 sec. Based on this the controller for the PI controlled mechanical input speed was set to give minimal overshoot of the dc supply bus voltage. The simulation for generator only operation is shown in Figures 4.6- 4.9. Figure 4.6 shows the commanded and actual speeds of generator only operation. Within the first second, the actual speed sags due to low dc bus voltage. After the generator begins to ramp up to rated speed, the generator is capable of supplying enough power to keep the voltage level needed by the BDC motor. Peak power supplied by the generator is (14N*m)*(290rad/sec) or 4.06kW.

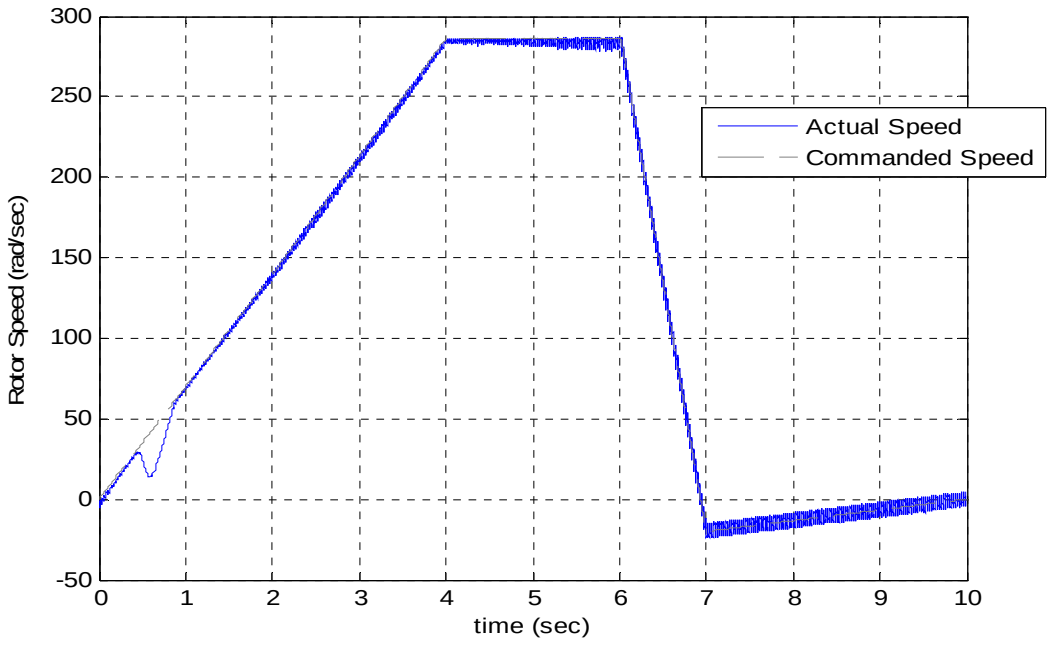

Figure 4.6. Generator only – rotor speed

The speed error starts at a time when both the mechanical load torque and the commanded speeds are relatively low. The rotor speed error peaks at a time when the dc supply bus voltage is lower than that needed by the BDC driver. After the generator has had sufficient time to ramp up to speed, the error is reduced. The mechanical load torque is shown in Figure 4.7.

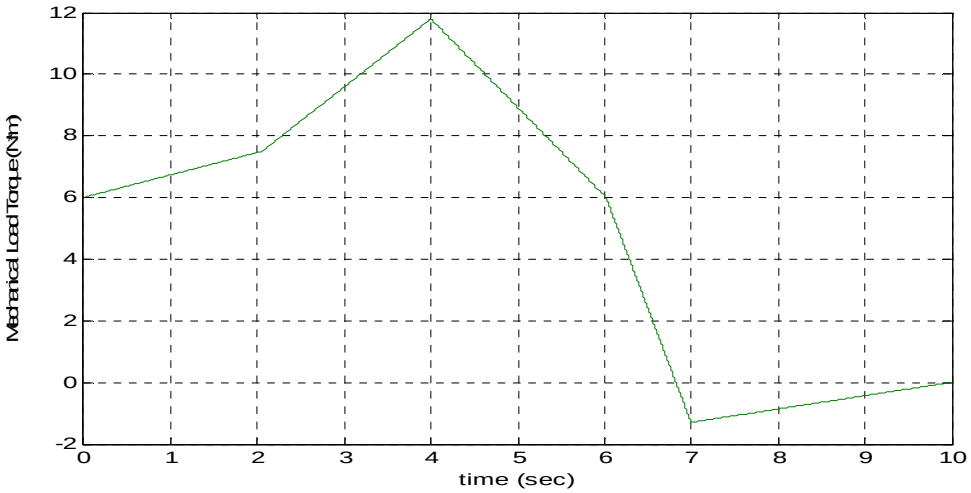

Figure 4.7. Generator only – mechanical load torque

Generator currents are shown in Figure 4.8. The generator supply current in Figure 4.8(a) shows the current supplied from the generator to the dc bus. The current never exceeds 100 A. The low-pass filtered supply current is shown in Figure 4.8(b). Filtered current contribution shows that the generator increases current injection into the dc bus during any voltage sag. The duty cycle of the boost converter is limited to keep supply currents to the dc bus limited.

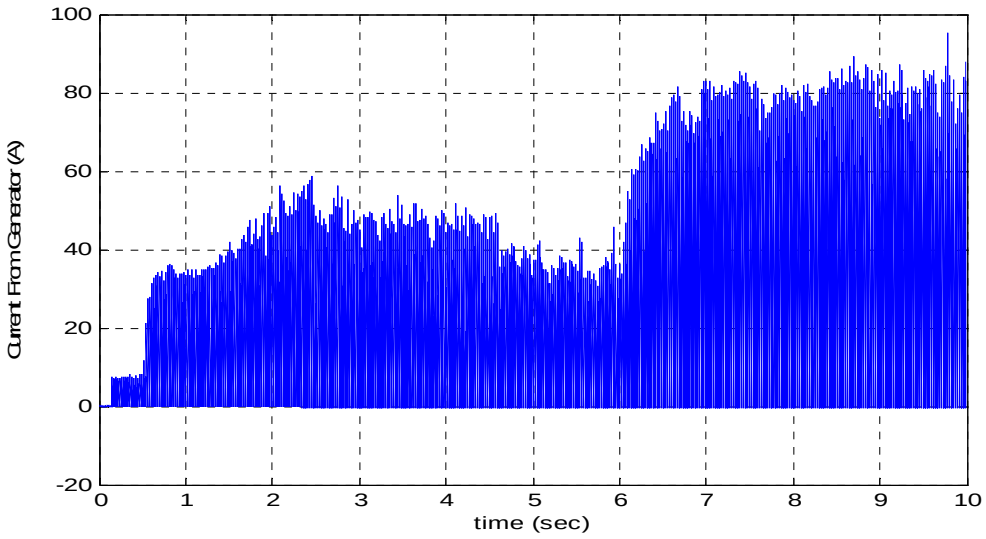

(a) Generator only - current contribution

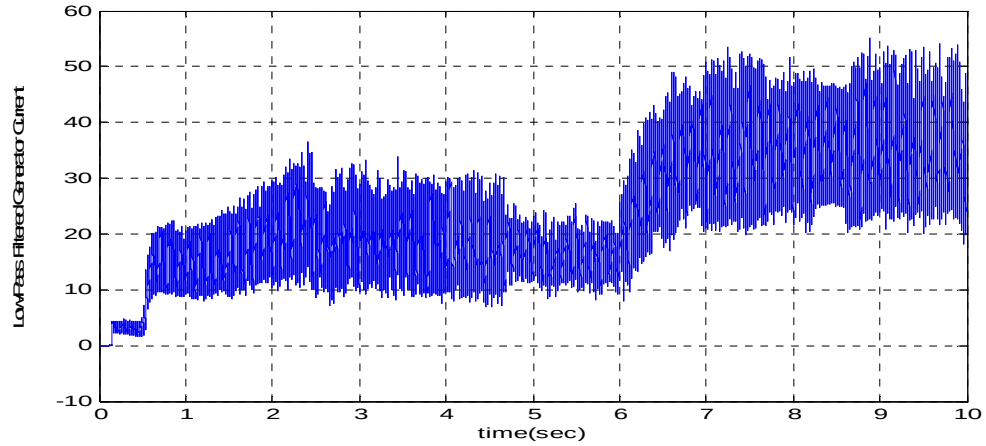

(b) Generator only – filtered current contribution
Figure 4.8. Currents

The voltage of the dc bus, shown in Figure 4.9, sags initially because the generator has not come up to speed. The initial voltage is due to the assumed initial charge of the dc bus capacitor to 160V. After the generator accelerates, the dc bus voltage stays nearly constant at slightly under 400V. The sag in voltage beginning at t = 6 sec. is due to desired dc bus voltage being reached. The generator then slows

down in speed, after which the generator must speed up to raise the bus dc voltage because power is still demanded from the BDC motor. This accounts for the larger current contributions from the generator towards the end of the simulation.

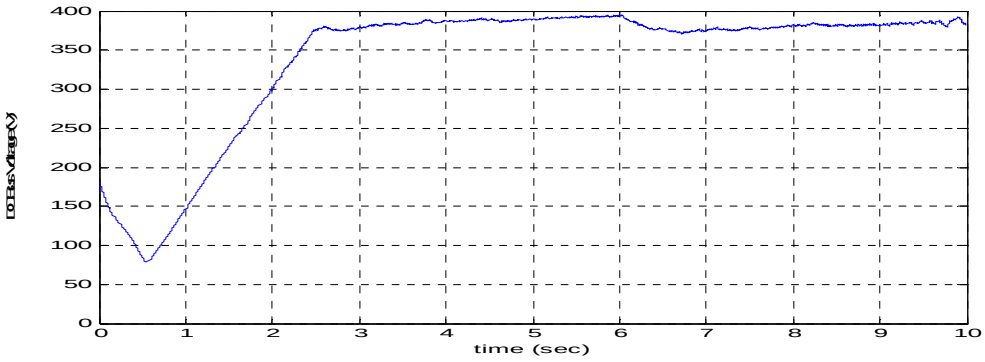

Figure 4.9. Generator only - dc bus voltage

4.3 GENERATOR AND ULTRA-CAPACITOR OPERATION

4.3.1 Low BDC Input Voltage-Low Mechanical Load Torque. This set of simulations considers the same commanded speeds and the same load torque that was considered in Sections 4.1 and 4.2. When both the ultra-capacitor and the generator are connected to the dc bus, the dc bus remains constant at around 200 V until the generator begins to inject current into the dc bus as shown in Figure 4.4. The error for the system is minimized and almost non-existent. The commanded and actual rotor speeds are shown in Figure 4.10 to be almost identical. The load torque of the system is the same as with the previous simulations as shown in Figure 4.11. The load peaks at a simulation time of 4 sec. with no effect on the actual rotor speed.

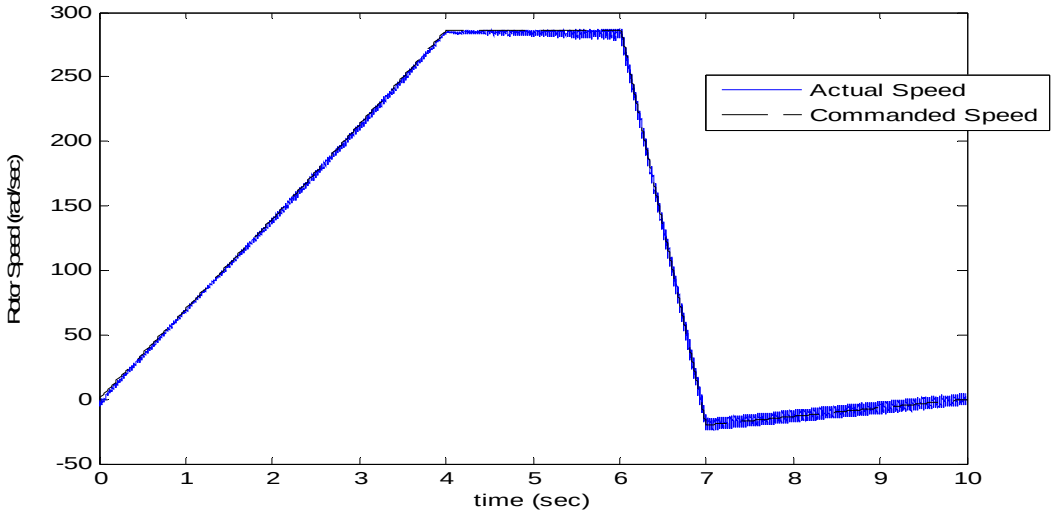

Figure 4.10. Generator and ultra-capacitor – rotor speed

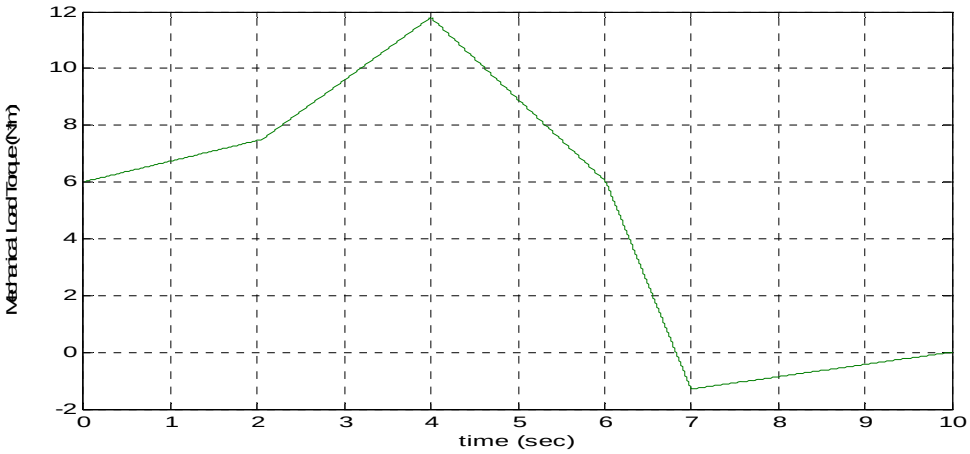

4.11. Generator and ultra-capacitor – mechanical load torque

Current contribution from the generator is shown in Figure 4.12(a). Low-pass filtered generator currents can be seen in Figure 4.12(b). Current values never exceed 100 A.

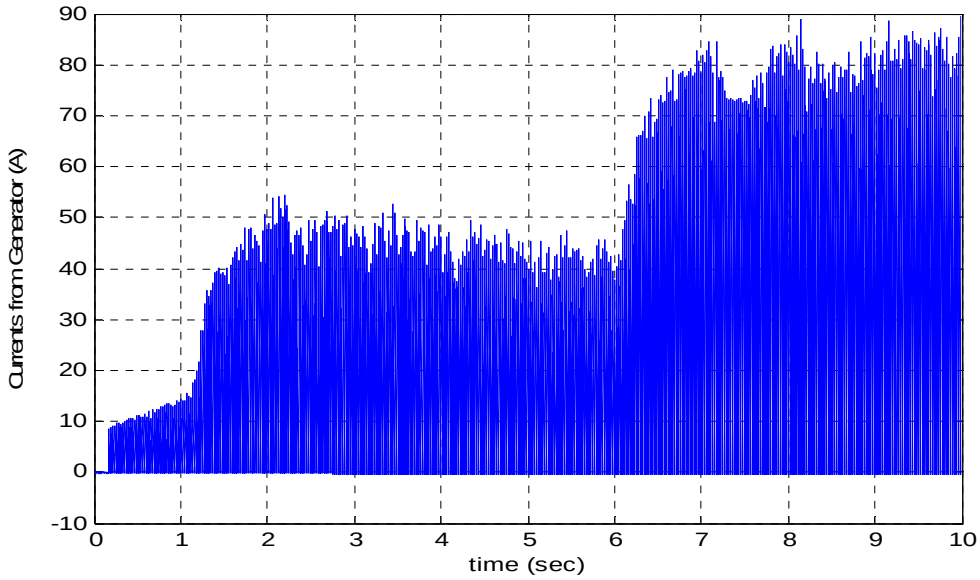

(a) Generator current contribution

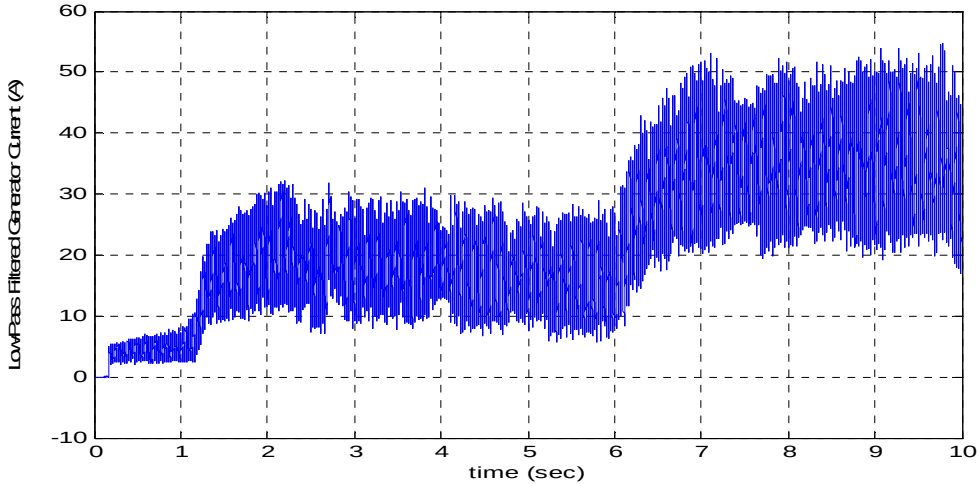

(b) Filtered generator current contribution
Figure 4.12. Generator and ultra-capacitor

Current contribution from the ultra-capacitor is shown in Figure 4.13(a). Low-pass filtered ultra-capacitor current is shown in Figure 4.13(b). Current is sent to the dc bus to keep the dc bus voltage near 200 V. The generator then contributes most of the current to the dc bus after it begins to ramp up to the rated speed.

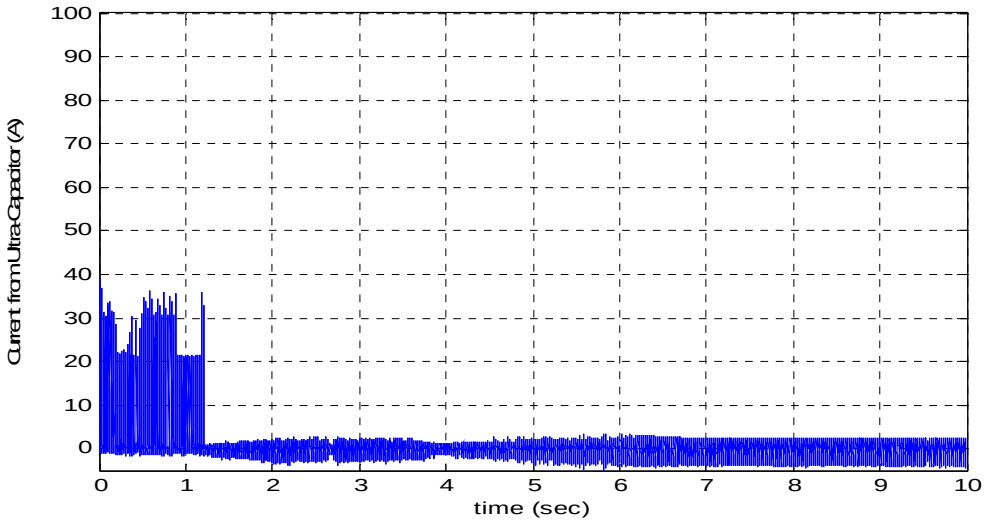

(a) Ultra-capacitor current contribution

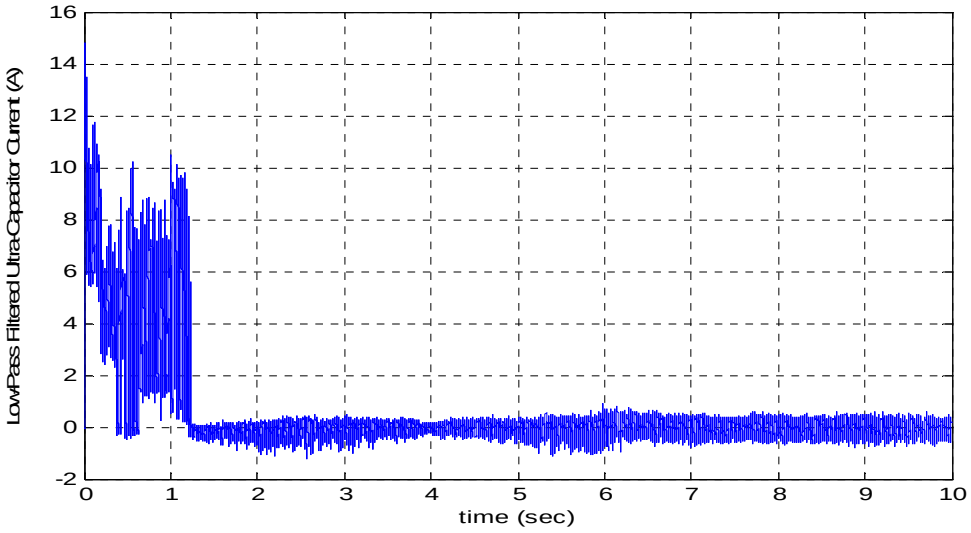

(b) Filtered ultra-capacitor current
Figure 4.13. Generator and ultra-capacitor

It can be seen in Figure 4.14 that the dc bus voltage does not have any significant sags. The voltage is kept close to 400 V regardless of system load. For approximately the first second of the simulation, the bus voltage is maintained by the

ultra-capacitor. At around 1.25 seconds the generator takes over and begins to supply more current to the load, and the generator keeps the bus voltage near 400 V.

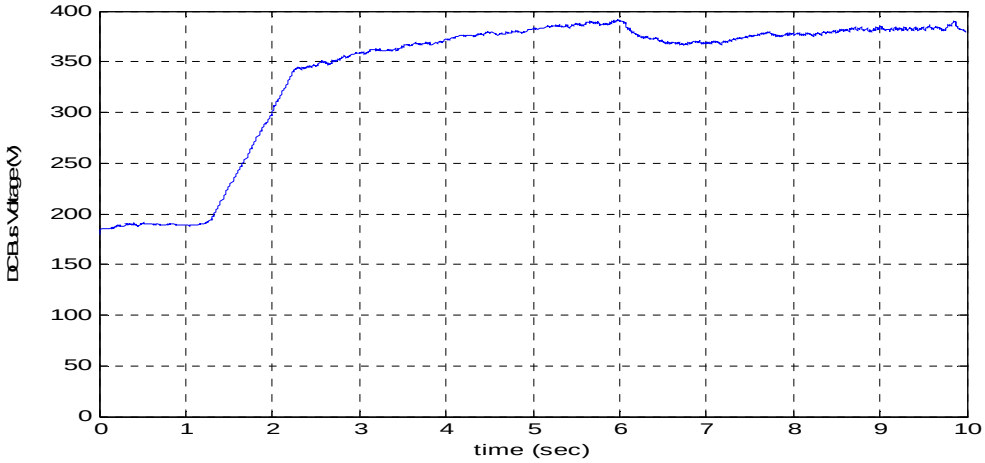

Figure 4.14. Generator and ultra-capacitor - dc bus voltage

4.3.2 Regenerative Operation. The system is also capable of regeneration if needed. When a low commanded speed and, more importantly, a large negative torque is applied to the BDC, the motor operates in generation mode supplying power to the dc bus. The bi-directional converter is controlled to charge the UC when a bus voltage of at least 385 V is reached. In Figure 4.15 it can be seen that the actual rotor speed is the same as the commanded rotor speed. The mechanical load torque is shown in Figure 4.16.

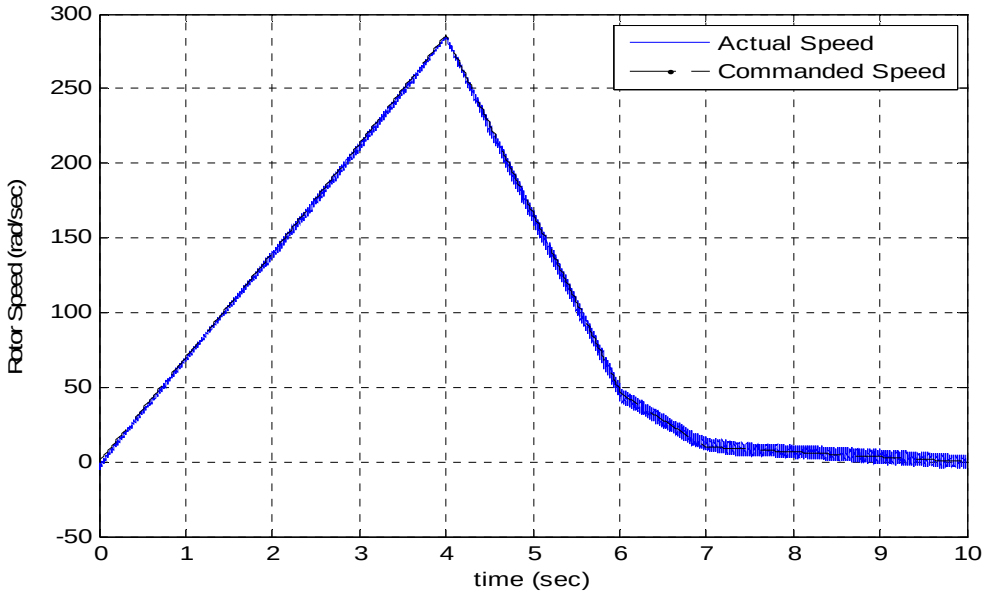

Figure 4.15. Regenerative braking – rotor speed

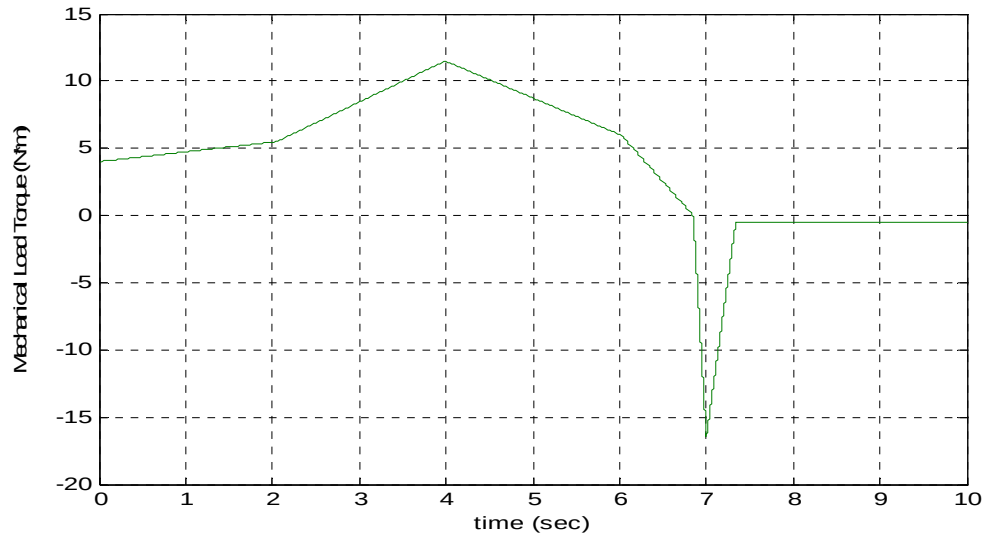

Figure 4.16. Regenerative braking – mechanical load torque

The currents from the ultra-capacitor are shown in Figure 4.17. It should be noted that initially when the negative mechanical torque peaks, the dc bus is

recharged. The small negative torque after the peak is what is responsible for the power regeneration and charging of the UC. Current is gradually increased as the commanded speed is relaxed.

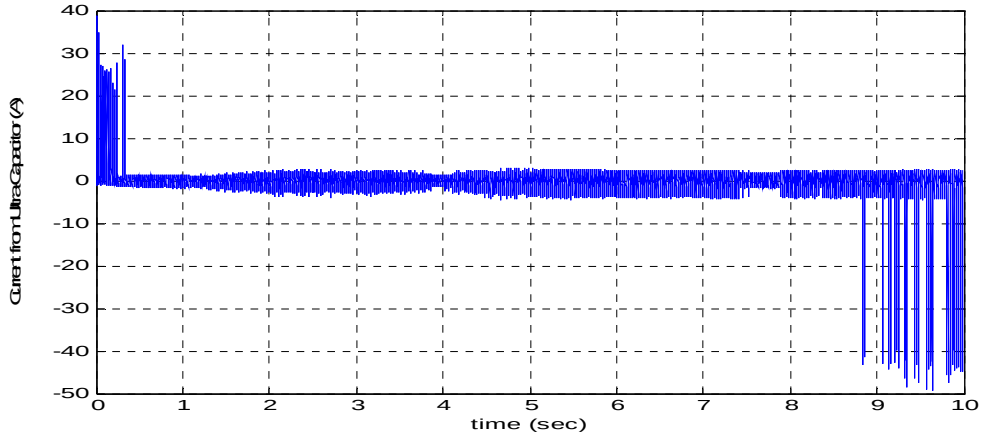

Figure 4.17. Regenerative braking – ultra-capacitor current

The dc bus voltage of the system is shown in Figure 4.18. The voltage is increased initially due ultra-capacitor performance. Towards the end of the simulation the dc bus voltage levels off at 385 V as the ultra-capacitor is charged.

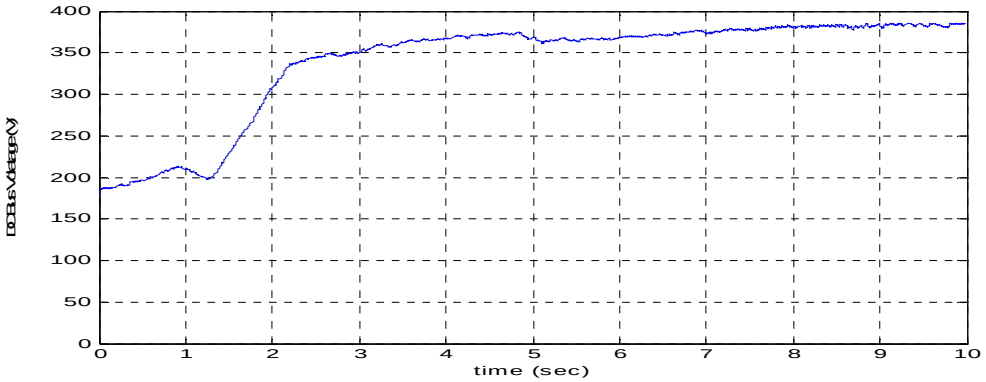

4.18. Regenerative braking - dc bus voltage

4.3.3 Regenerative Operation – Reverse Speed Direction. When the system has a commanded speed in the reverse direction, the performance of the system was similar to the previous examples. There was relatively little error in the overall system rotor speed, as seen in Figure 4.19. The UC compensated for the delay in generator operation and the system followed the commanded speeds. The commanded speed was made negative going to near the rated speed. The speed was then commanded to a positive value, and then it was set to zero. The mechanical load torque was the same as the previous simulation as seen in Figure 4.20.

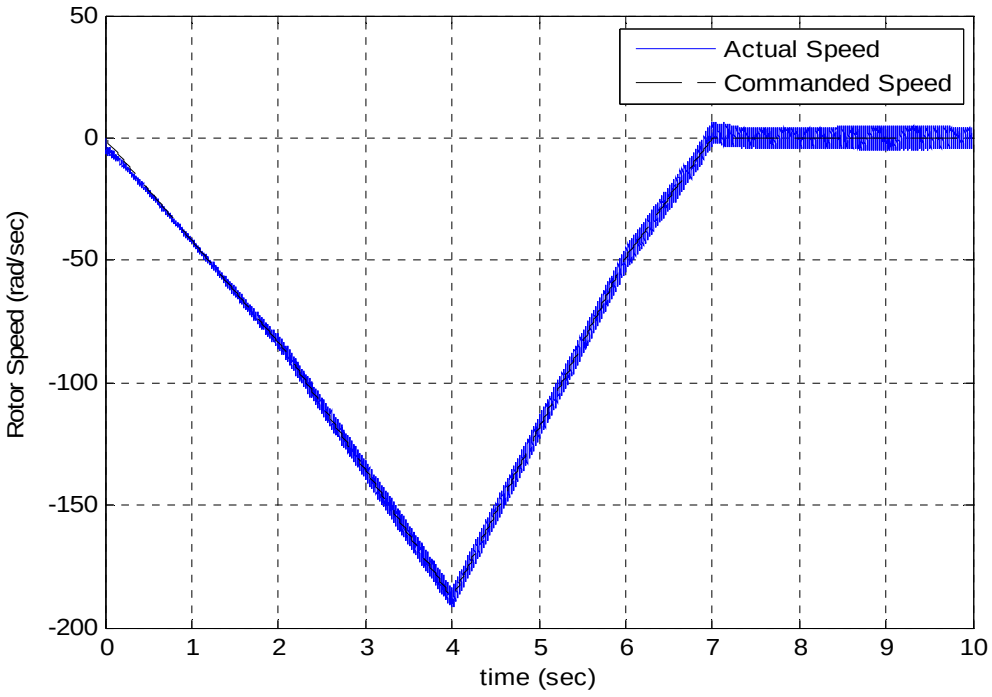

Figure 4.19. Regenerative braking, negative rotor speed – rotor speed

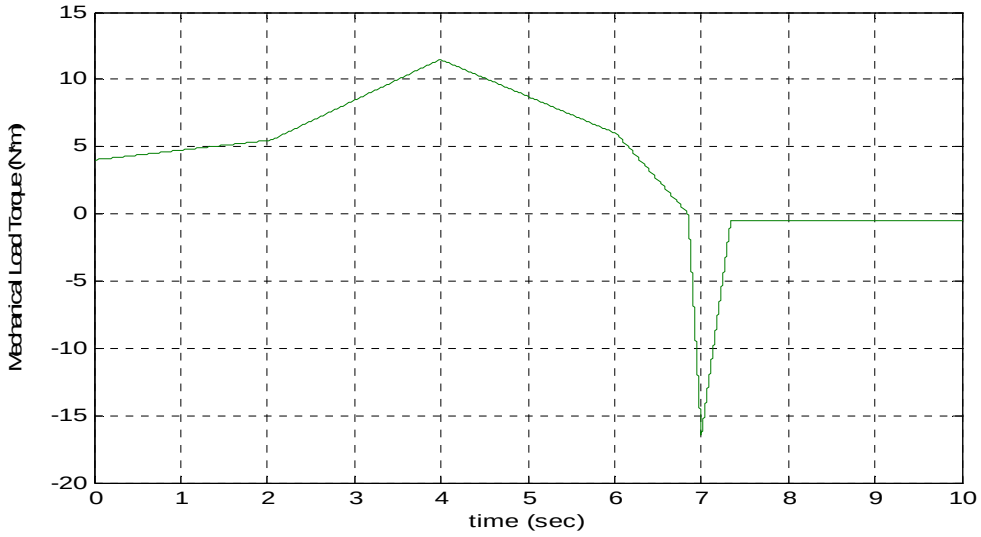

Figure 4.20 Regenerative braking, negative rotor speed - mechanical load torque

Figure 4.21 shows the currents from the ultra-capacitor. Initially the ultra-capacitor is used to increase the dc bus voltage. After a large negative spike in the mechanical load of the BDC motor, the ultra-capacitor begins to recharge.

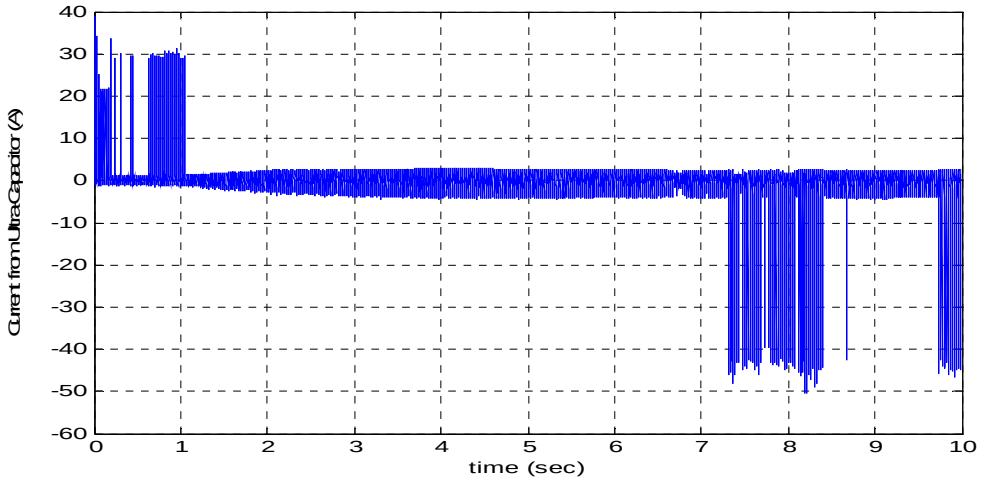

Figure 4.21 Regenerative braking, negative rotor speed – ultra-capacitor current

The dc bus voltage is able to move to 385 V quicker due to lower power demands of the BDC motor. The voltage of the dc bus is shown in Figure 4.22. The additional voltage from a smaller load causes the bi-directional converter to enter buck mode sooner and the ultra-capacitor begins to recharge beginning at around t = 7.3 sec.

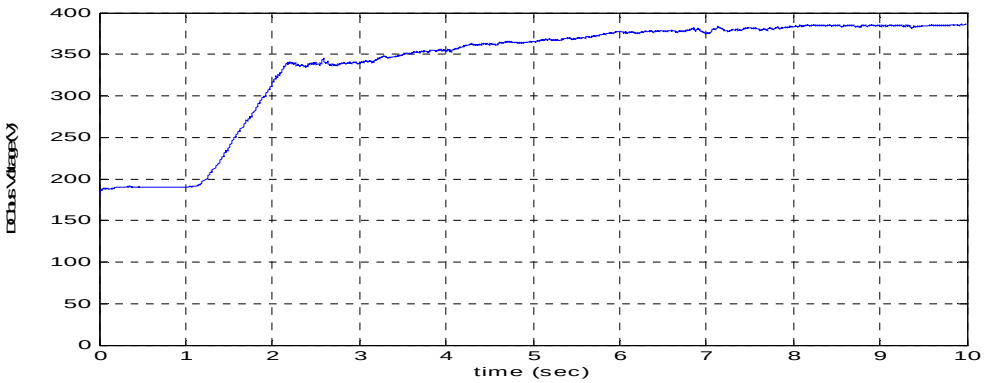

Figure 4.22 Regenerative braking, negative rotor speed – dc bus voltage

4.4 DISCUSSION

Simulations were completed for different power sources in a hybrid electric vehicle. The simulations show that the use of both power sources in the system provides optimal performance of the system by using the advantages of both inputs to maintain a steady dc input voltage. The ultra-capacitor will help maintain a minimum voltage of around 200 V for low power applications, and the generator supplied power during peak power conditions. Regeneration is possible by coordinating the bi-directional converter to divert power during periods where the dc bus voltage exceeds a maximum dc bus value. Currents were kept within an acceptable range by

limiting the duty cycle of the power MOSFETs in the boost mode and these current readings seem to be consistent with BDC motor drives used in the past. These simulations showed how performance of the BDC drive was enhanced by the control of power flow to and from the dc supply bus.

5. CONCLUSION AND FUTURE WORK

One type of a power system on board a hybrid vehicle was presented for consideration that included two power inputs to a dc bus of a BDC drive. It was observed that, for a hybrid power system consisting of a PMSM and an ultra-capacitor in a series hybrid configuration powering a BDC motor, the BDC motor can be controlled and some errors can be reduced or eliminated by the use of the ultra-capacitor to complement the generator. Performance of the BDC motor was dependent on the amount of current that could be injected into the dc bus to maintain a minimum voltage for the demands of the BDC motor.

The BDC motor was capable of operating effectively in forward and reverse rotor speeds at different torque levels. It was also possible to recapture excess energy on the dc bus voltage by operating the bi-directional DC-DC converter to re-charge the UC. The control of the system was implemented through a set of power electronic converters to the dc bus.

The operation of the BDC motor was shown to be effective as long as enough power was supplied to the dc bus. Occasionally the dc bus voltage would dip to a level where the BDC hysteresis controlled driver could not operate properly either at low speed, low torque or high speed, high torque.

The main limitation of the effectiveness of the generator was the assumption that the generator would take time to ramp up to rated speed. Since the output of the PMSM generator is dependent on input rotor speed, careful consideration has to be taken when designing the control of the generator. The current injected into the dc

bus was also limited by the slow switching frequencies that were required to run the simulation.

The limitation of the ultra-capacitor is that when the current supply levels are kept low, it can only supply limited power to the system. The limitations of the simulations are due to the inability to provide larger switching frequencies of the DC-DC converters. Unfortunately, the combined system requires a very long time to run and decreasing the step size of the solver in discrete mode would take hours to run a 20 second simulation. Nonetheless, the ultra-capacitor in the system can supply current quickly, but very large currents would be required to operate the BDC motor drive under normal operating conditions. Sustained use of the ultra-capacitor alone would eventually drain the ultra-capacitor voltage.

One BDC motor is enough for limited operation of a light-weight vehicle. More BDC motors could be attached to the dc bus, but more power would have to be supplied to the dc bus from the different power sources. This motor would be sufficient for the operation of a small vehicle.

Future work for this thesis would be to develop and incorporate other forms of energy storage, such as a battery or fly-wheel, and other forms of power management and make the system more effective at higher power levels by incorporating simulations that can handle higher switching frequencies of the power electronic converters. Also, a more complete model that takes into account vehicle performance and incorporates fuel efficiency should be considered a more practical application.

APPENDIX

Circuit Information

PMSM Generator Data:

3-phase rectifier diodes

Parameter	**Value**
On-state resistance	0.001 ohms
Forward Voltage	0.8 V
Snubber Resistance	500 ohms
Snubber Capacitance	250×10^{-9} F

Generator PI control

Parameter	**Value**
K_p	1
K_i	1
Output Voltage Setpoint When ON	200 V

Converter Data

Generator Boost Converter

Parameter	Value
Inductor	5 μH
Mosfet	On-state resistance: 0.1 ohm Internal diode resistance: 0.01 ohm Snubber Resistance: 0.1 Mohm
Diode	On-state resistance: 0.001 ohms Forward voltage: 0.8 V Snubber Resistance: 500 ohms Snubber Capacitance: 250 nF
Duty Cycle	Fixed: 0.1

Bi-Directional Boost Converter

Parameter	**Value**
Inductor	300 μH
Mosfet	On-state resistance: 0.1 ohm Internal diode resistance: 0.01 ohm Snubber Resistance: 0.1 Mohm
Inductor	5 μH
Duty Cycle	PI controlled : Boost Limited to: 0 - 0.01 Buck Limited to: 0 - 0.9

BIBLIOGRAPHY

[1] http://www.maxwell.com/ultracapacitors/index.asp, Maxwell Technologies: Ultracapacitors, Micro electronics for Space, High Voltage Capacitors, Mar. 20, 2007.

[2] S.S. Williamson, A. Khaligh, S. C. Oh, and A. Emadi, "Impact of energy storage device selection on the overall drive train efficiency and performance of heavy-duty hybrid vehicles," IEEE Conference Vehicle Power and Propulsion, pp., 7-9 Sept. 2005.

[3] J. Gan, K.T. Chau, Y. Wang, C.C. Chan, and J.Z. Jiang, "Design and analysis of a new permanent magnet brushless DC machine," IEEE Transactions on Magnetics, volume 36, Issue 5, Part 1, pages 3353 – 3356, Sept 2000.

[4] http://www.maxwell.com/pdf/uc/datasheets/mc_power_series_48_1009365_rev2.pdf March 26, 2007

[5] K.P. Yalamanchili and M. Ferdowsi, "Review of multiple input DC-DC converters for electric and hybrid vehicles," 2005 IEEE Conference on Vehicle Power and Propulsion, pages 160 – 163, 7-9 Sept. 2005.

[6] G. Maggetto and J. Van Mierlo, "Electric and electric hybrid vehicle technology: a survey," IEE Seminar Electric, Hybrid and Fuel Cell Vehicles, pp. 1/1 – 111, 11 April 2000.

[7] J. Liu and H. Peng, "Control optimization for a power-split hybrid vehicle," American Control Conference, 2006, Page(s):6 pp., 14-16 June 2006.

[8] C.C. Chan and Y.S. Wong, "The state of the art of electric vehicles technology," The 4th International Power Electronics and Motion Control Conference, Volume 1, pp. 46 - 57 , 2004.

[9] K. Kawashima, Y. Hori, and T. Uchida, "Stabilizing control of vehicle motion using small EV driven by ultra capacitor," 32nd Annual Conference of IEEE Industrial Electronics Society, 2005. , pp. 6 pp., 6-10 Nov. 2005.

[10] S.S. Williamson, A. Khaligh, S.C. Oh, and A. Emadi, "Impact of energy storage device selection on the overall drive train efficiency and performance of heavy-duty hybrid vehicles," 2005 IEEE Conference Vehicle Power and Propulsion, pp. 10, 7-9 Sept. 2005.

[11] Z.M. Salameh, M.A. Casazza, and W.A. Lynch "A mathematical model for lead-acid batteries," IEEE Transactions on Energy Conversion, Volume 7, Issue 1, pp. 93 – 98, March 1992.

[12] M. Chen and G.A. Rincon-Mora, "Accurate electrical battery model capable of predicting runtime and I-V performance," IEEE Transactions on Energy Conversion, Volume 21, Issue 2, pp. 504 – 511, June 2006.

[13] The MathWorks, Inc. - Matlab, "Permanent Magnet Synchronous Machine," 1994-2005.

[14] K.A. Corzine, S.D. Sudhoff, and H.J. Hegner, "Analysis of a current-regulated brushless DC drive," IEEE Transactions on Energy Conversion, Volume 10, Issue 3, pp. 438 – 445, Sept. 1995.

[15] F. Crescimbini, A. Di Napoli, L. Solero, and F. Caricchi, "Compact permanent-magnet generator for hybrid vehicle applications," Conference Record of the 38th IAS Annual Meeting, Volume 1, pp. 576 - 583 vol.1, 12-16 Oct. 2003.

[16] A. Lidozzi and L. Solero, "Power balance control of multiple-input DC-DC power converter for hybrid vehicles" 2004 IEEE International Symposium on Industrial Electronics, Volume 2, pp. 1467 – 1472, 4-7 May 2004.

[17] Dr. Keith Corzine, "EE-353, Power Electronics Class Notes," University of Missouri-Rolla. Winter Semester, 2007

VITA

James Jenkins was born in Fort Campbell, KY on March 19, 1981. He graduated from Francis Howell North High School and then attended UMR receiving his B.S. degree in Electrical Engineering in May 2004. He returned to UMR in 2005 to work on his M.S. in Electrical Engineering with an emphasis in power. His interests include power electronics and programmable logic controllers. He plans to work as an engineer in industry and then pursue a degree in business administration. He received his M.S. in May 2007.